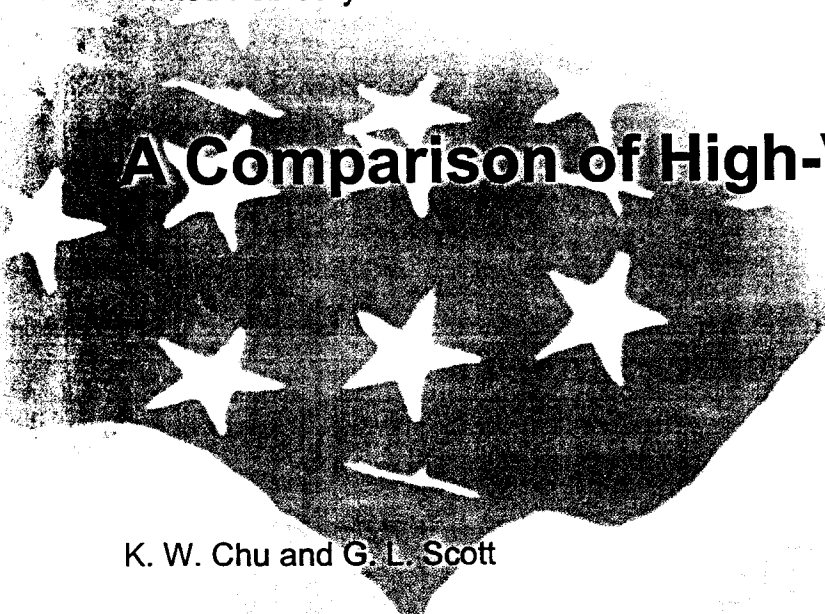


# SANDIA REPORT

SAND99-0154

Unlimited Release

Printed February 1999



## A Comparison of High-Voltage Switches

K. W. Chu and G. L. Scott

Prepared by  
Sandia National Laboratories  
Albuquerque, New Mexico 87185 and Livermore, California 94550

Sandia is a multiprogram laboratory operated by Sandia Corporation,  
a Lockheed Martin Company, for the United States Department of  
Energy under Contract DE-AC04-94AL85000.

Approved for public release; further dissemination unlimited.



Issued by Sandia National Laboratories, operated for the United States Department of Energy by Sandia Corporation.

**NOTICE:** This report was prepared as an account of work sponsored by an agency of the United States Government. Neither the United States Government, nor any agency thereof, nor any of their employees, nor any of their contractors, subcontractors, or their employees, make any warranty, express or implied, or assume any legal liability or responsibility for the accuracy, completeness, or usefulness of any information, apparatus, product, or process disclosed, or represent that its use would not infringe privately owned rights. Reference herein to any specific commercial product, process, or service by trade name, trademark, manufacturer, or otherwise, does not necessarily constitute or imply its endorsement, recommendation, or favoring by the United States Government, any agency thereof, or any of their contractors or subcontractors. The views and opinions expressed herein do not necessarily state or reflect those of the United States Government, any agency thereof, or any of their contractors.

Printed in the United States of America. This report has been reproduced directly from the best available copy.

Available to DOE and DOE contractors from  
Office of Scientific and Technical Information  
P.O. Box 62  
Oak Ridge, TN 37831

Prices available from (703) 605-6000  
Web site: <http://www.ntis.gov/ordering.htm>

Available to the public from  
National Technical Information Service  
U.S. Department of Commerce  
5285 Port Royal Rd  
Springfield, VA 22161

NTIS price codes  
Printed copy: A03  
Microfiche copy: A01



SAND99-0154  
Unlimited Release  
Printed February 1999

# A COMPARISON OF HIGH-VOLTAGE SWITCHES

K. W. Chu and G. L. Scott  
Firing Set and Contact Fuze Department  
Sandia National Laboratories  
P.O. Box 5800  
Albuquerque, NM 87185-0501

## **Abstract**

This report summarizes our experience in testing high-voltage switches that must have fast turn-on, low inductance, and low resistance. Our work was directed at fuze applications, but the information is relevant to any capacitor-discharge circuit where a high peak current and a rapid rate of increasing current (large  $dI/dt$ ) are of paramount importance. This report describes our test techniques and discusses the strengths and weaknesses of three switch technologies: gas, vacuum, and semiconductors.

## **Acknowledgments**

The authors thank Terry Ericson of the Office of Naval Research and Dr. Victor Temple of Silicon Power Corporation for providing MCT switches. We also thank Gordon Boettcher of Sandia National Laboratories for providing vacuum switches.

## Contents

Nomenclature .....	8
Introduction .....	9
Switch Testing.....	9
Pulse-Life Test.....	9
Switching-Performance Test.....	12
Gas Switches .....	15
First-Shot Effect.....	17
Degradation of Static-Breakdown Voltage .....	19
Operating Voltage Range.....	23
Triggering Mode .....	26
Switch Aging .....	27
Hybrid Switch .....	28
Vacuum Switches.....	30
First-Shot Effect in a Vacuum Switch .....	31
Low-Temperature and Switch Contamination.....	32
TAD Stability and Residual Gas.....	34
Early Isolated Hold-Off Failures.....	37
Gap Erosion and Metal Deposition.....	38
Semiconductor Switches .....	39
MCT Overview .....	39
N-MCT Stability .....	40
N-MCT Leakage .....	43
Gate Protection.....	44
Summary .....	47
References .....	51

## Figures

Figure 1. Definition of TAD and TAD2.....	11
Figure 2. Low Impedance Test Circuit.....	12

Figure 3. Voltage and Current Phase Shift.....	13
Figure 4. Voltage Corrected for Stray Inductance.....	14
Figure 5. Switch Turn-On Resistance .....	14
Figure 6. Gas Switch .....	15
Figure 7. Relationship of Gas and Vacuum Switches.....	16
Figure 8. SBV Stability at Low-Current Pulse.....	18
Figure 9. First-Shot Effect in a Gas Overvoltage Gap .....	19
Figure 10. SBV Degradation at High-Current Pulse.....	20
Figure 11. SBV Degradation and Gas Fill.....	21
Figure 12. Isolated-SBV Anomaly .....	22
Figure 13. Gas Release by Heating .....	23
Figure 14. TAD2 and Operating Voltage.....	24
Figure 15. TAD and Operating Voltage .....	25
Figure 16. Trigger-Break Variability.....	25
Figure 17. TAD2 and Operating Mode .....	26
Figure 18. TAD and Operating Mode. ....	27
Figure 19. Aging of a Gas Switch .....	28
Figure 20. Hybrid Switch .....	29
Figure 21. Hybrid Switch Pulse-Life Test.....	29
Figure 22. Vacuum Switch.....	30
Figure 23. First-Shot Effect in Vacuum Switches.....	31
Figure 24. TAD in Uncontaminated Switch.....	32
Figure 25. TAD in Contaminated Switch.....	33
Figure 26. Peak Current in Contaminated Switch.....	33
Figure 27. Residual Gas and Delay Instability .....	35
Figure 28. Gas Removal.....	36
Figure 29. Residual Gas and Current Pulse Shape .....	36
Figure 30. Isolated Hold-Off Failure on Shot 14 .....	37
Figure 31. Erosion and Deposition.....	38
Figure 32. N-MCT Diagram.....	40
Figure 33. TAD Histogram. ....	41

Figure 34. Peak Current Temperature .....	41
Figure 35. TAD versus Temperature.....	42
Figure 36. Peak Current versus Temperature .....	42
Figure 37. Leakage Current versus Temperature .....	43
Figure 38. Leakage Current versus Voltage .....	44
Figure 39. N-MCT Trigger Circuit.....	45
Figure 40. Gate Overvoltage in Low-Impedance Trigger Circuit .....	45
Figure 41. Gate Protected in High-Impedance Trigger Circuit .....	46
Figure 42. Switching Performance at 1000 V .....	48
Figure 43. Switching Performance at 3000 V .....	48

**Tables**

Table 1. Switch Comparisons.....	47
Table 2. Switch Inductance, Turn-On Time, and Resistance .....	49

## Nomenclature

CVR	current-viewing resistor
DoD	Department of Defense
DOE	Department of Energy
MOS	metal oxide semiconductor
MOSFET	metal oxide semiconductor field-effect transistor
MCT	MOS-controlled thyristor
RLC	resistance, inductance, and capacitance
SBV	static-breakdown voltage
SCR	silicon-controlled rectifier
TAD	Trigger Anode-current Delay
TAD2	Trigger-break to Anode-current Delay
$dI/dt$	rate of change of current: units of current per unit time
$dV/dt$	rate of change of trigger voltage: units of voltage per unit time

# A Comparison of High-Voltage Switches

## Introduction

This report summarizes our work on high-voltage switches during the past few years. With joint funding from the Department of Energy (DOE) and the Department of Defense (DoD), we tested a wide variety of switches to a common standard. This approach permitted meaningful comparisons between disparate switches. Most switches were purchased from commercial sources, though some were experimental devices. For the purposes of this report, we divided the switches into three generic types (gas, vacuum, and semiconductor) and selected data that best illustrates important strengths and weaknesses of each switch type. Test techniques that indicate the state of health of the switches are emphasized. For example, a good indicator of residual gas in a vacuum switch is the systematic variation of the switching delay in response to changes in temperature and/or operating conditions. We believe that the presentation of this kind of information will help engineers to select and to test switches for their particular applications.

Our work was limited to switches capable of driving slappers. Also known as *exploding-foil initiators*,<sup>1</sup> slappers are detonators that initiate a secondary explosive by direct impact with a small piece of matter moving at the detonation velocity (several thousands of meters per second). A slapper is desirable for enhanced safety (no primary explosive), but it also places extra demands on the capacitor-discharge circuit to deliver a fast-rising current pulse (greater than 10 A/ns) of several thousand amperes. The required energy is substantially less than one joule; but this energy is delivered in less than one microsecond, taking the peak power into the megawatt regime. In our study, the switches operated in the 1 kV to 3 kV range and were physically small, roughly 1 cm<sup>3</sup> or less. Although a fuze functions only once in actual use, multiple-shot capability is important for production testing and for research work. For this reason, we restricted this report to multiple-shot switches. Furthermore, our work included only switches with submicrosecond timing precision, thereby excluding mechanical switches.

## Switch Testing

### Pulse-Life Test

In a pulse-life test, the switch repeatedly discharges a capacitor for a specified number of shots or until the switch fails. Gas and vacuum switches suffer irreversible damage with each shot, and it is practical to test them until failure. A semiconductor

switch has no comparable wear-out mechanism; and unless extra stress is applied, it is impractical to test a semiconductor switch until failure. There are two types of outright failures in a pulse-life test: no-fire and hold-off. In a no-fire failure, the switch does not close after receiving the required trigger. In a hold-off failure (also called a *prefire*), the switch closes without having received a trigger.

Besides detecting outright failures, the pulse-life test monitors several parameters to measure switch performance. For example, we monitored the current pulse by measuring the rate at which the current is changing ( $dI/dt$ ), the peak current, and the total electrical charge (integral of the absolute current over time). By measuring the trigger-break voltage and the slope of the trigger voltage ( $dV/dt$ ), we monitored the trigger pulse. And finally, we monitored the switching delay by measuring the time interval between the trigger pulse and the current pulse. Automated equipment is a necessity for pulse-life testing because the amount of data is large, and the test of a single switch may span a few days.

Switching delay is an especially sensitive indicator of switch stability. Gas and vacuum switches, for example, always have measurable timing jitter at 1 ns resolution. The electric arc slightly alters these switches on each shot, introducing some inherent randomness into the switching delay of successive shots. Semiconductor switches, on the hand, have little timing jitter at 1 ns resolution because they are solid state. Temperature or unit-to-unit variation will limit the timing accuracy of a semiconductor switch. Figure 1 shows the two delays that were measured in our pulse-life tests. The Trigger Anode-current Delay (TAD) denotes the time from the start of the trigger pulse to the start of the anode current. TAD2 is the delay from trigger-break to the start of the anode current. Trigger-break is the abrupt drop of the trigger voltage caused by electrical breakdown between the trigger pin and the adjacent electrode; trigger-break is applicable only to gas and vacuum switches. Thus TAD2 is undefined for semiconductor switches because they have no trigger-break. Gas and vacuum switches usually have a well-defined trigger-break; but there are occasions when the trigger voltage does not abruptly drop, resulting in a poorly defined TAD2. Some switch manufacturers quote TAD2 as the delay of their switch. This interpretation can be misleading because, from a system perspective, TAD is the relevant parameter for measuring timing precision.

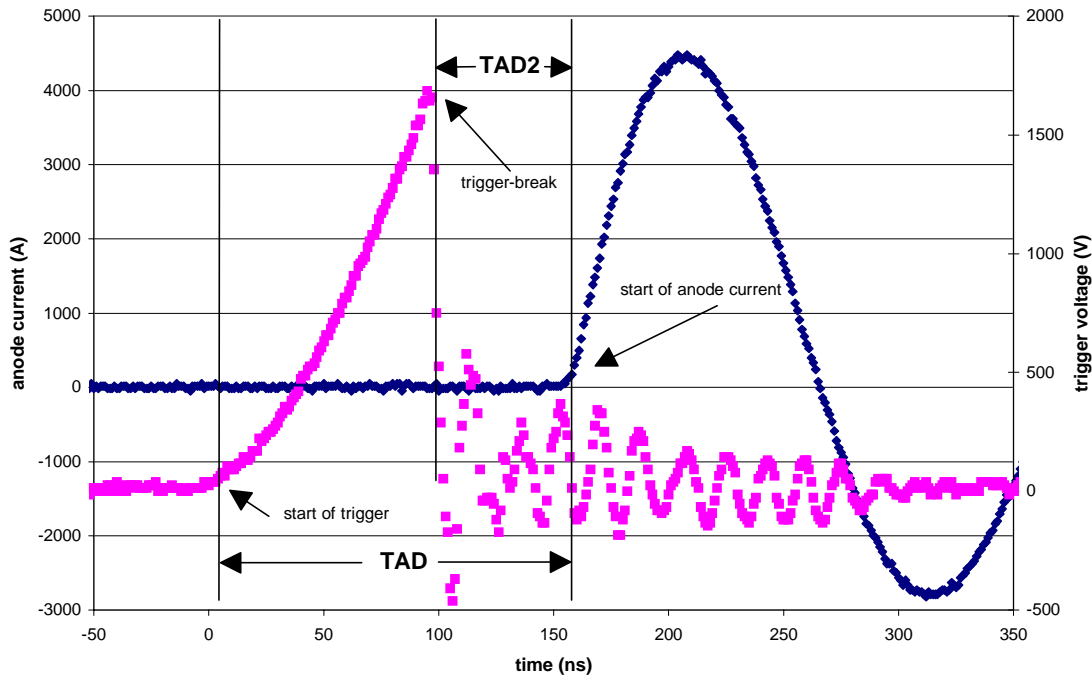


**Figure 1. Definition of TAD and TAD2.** TAD is the delay from the start of the trigger pulse to the start of the anode current. TAD2 is the delay from trigger-break to the start of the anode current. TAD2 is applicable to only vacuum and gas switches in which the trigger voltage abruptly collapses.

In a pulse-life test, the switching delay is measured at a constant rate of fire (typically a few shots per minute). Under actual-use conditions, the switch is idle from months to perhaps many years, and then the fuze must work one time. Some vacuum and gas switches behave differently on the first shot after an extended period of idleness when compared to repetitive shots taken minutes apart; we call this a *first-shot effect*. The statistics of switching delay obtained from pulse-life tests will not accurately represent actual performance if the switch exhibits a first-shot effect. In any system where switching delay is a critical parameter, vacuum and gas switches should be tested for a first-shot effect.

Hold-off and no-fire failures are infrequent events, and the pulse-life test must provide a high level of confidence that all true failures are detected and that all detected failures are true. At a minimum during a pulse-life test, we operated two digitizing scopes. The trigger source of scope-1 was the switch-trigger signal, and the trigger source of scope-2 was the anode-current signal. The primary purpose of scope-2 was to detect hold-off failures. Scope-1 was the normal data acquisition digitizer, and it captured the anode-current and the trigger pulse for each normal shot. If scope-1 showed no anode-current pulse and scope-2 did not trigger, a true no-fire failure would be confirmed. If scope-1 showed no anode-current pulse, but a normal current pulse triggered scope-2, a long delay would be confirmed. Presumably, the current pulse occurred after the sweep of scope-1. In a true hold-off failure, scope-2 must trigger, and there must be no trigger voltage prior to the discharge current pulse. Scope-1 may or may not trigger, depending

on how much signal is coupled from the discharge current pulse to the trigger pin. This type of setup is essential for vacuum and gas switches that occasionally experience isolated failures or very long delays.

## Switching-Performance Test

We compared the turn-on characteristics of the switches by firing them in the same low-impedance RLC circuit (see Figure 2). The rationale for using a low-impedance circuit was to maximize the effect of the switch; i.e., the inductance and resistance of the circuit (excluding the switch) should be as small as possible compared to the switch. As a consequence, the discharge current will depend more on the switch than the test circuit.

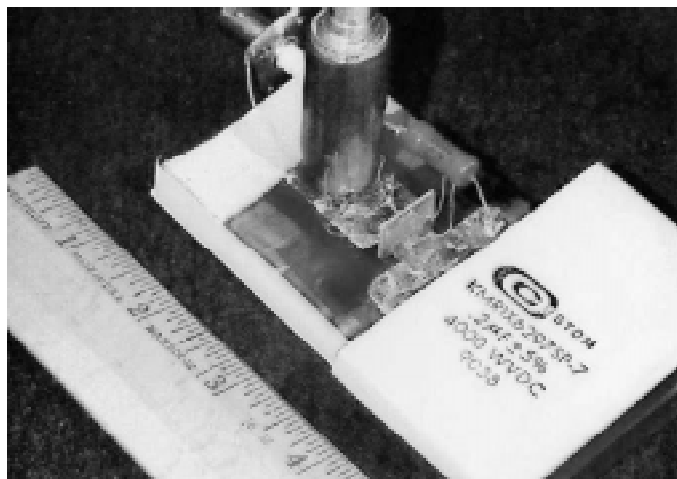


**Figure 2. Low-Impedance Test Circuit.** This photograph shows the RLC circuit that was used to compare switching performance. The  $5\text{ m}\Omega$  current-viewing resistor (CVR), the vertical cylindrical object, is connected by a stripline to the  $0.2\text{ }\mu\text{F}$  low-inductance capacitor. In the absence of a switch, the total circuit inductance is  $3.6\text{ nH}$  ( $\pm 10\%$ ), and the total resistance is  $20\text{ m}\Omega$  ( $\pm 50\%$ ). In this photograph, the switch, an N-MCT semiconductor, is located between the CVR and the capacitor.

The performance of a switch is determined by three parameters: inductance, turn-on speed, and resistance. We determined switch inductance by measuring the difference in the ring period with and without the switch in the test circuit. A few switches with high resistance did not ring, and their inductance could not be measured by this technique. The switch inductance depends in part on how the switch is physically mounted in the test circuit. In our tests, we mounted the switches in a manner to minimize the inductance. Other mounting configurations may add more inductance than what is quoted in this report.

To measure the resistance of the switch, the voltage waveform must be corrected for stray inductance. For some switches, the voltage probe leads can be placed at positions where the stray inductance is negligible. In the typical switch, it is not possible to avoid some stray inductance, and the zero-current and zero-voltage crossings do not match (see

Figure 3). The other complication is that the voltage probe compensation is not perfect, and there is uncertainty about the zero-volt baseline. We used an argument based on internal consistency to find the stray inductance. At each of the first two zero-current points, we calculate the stray inductances ( $L1$  and  $L2$ ) by dividing the voltage by  $dI/dt$ . In general,  $L1$  and  $L2$  are not equal, but shifting the zero-volt baseline can equalize  $L1$  and  $L2$ . Imperfect voltage-probe compensation justifies shifting the zero-volt baseline. The stray inductance is taken to be the equalized value of  $L1$  and  $L2$ . The voltage waveform is now corrected by subtracting the voltage drop across the stray inductance. The zero-crossings of the current and corrected voltage waveforms will match (see Figure 4), and the resistance as a function of time is determined by dividing the corrected voltage by the current (see Figure 5).

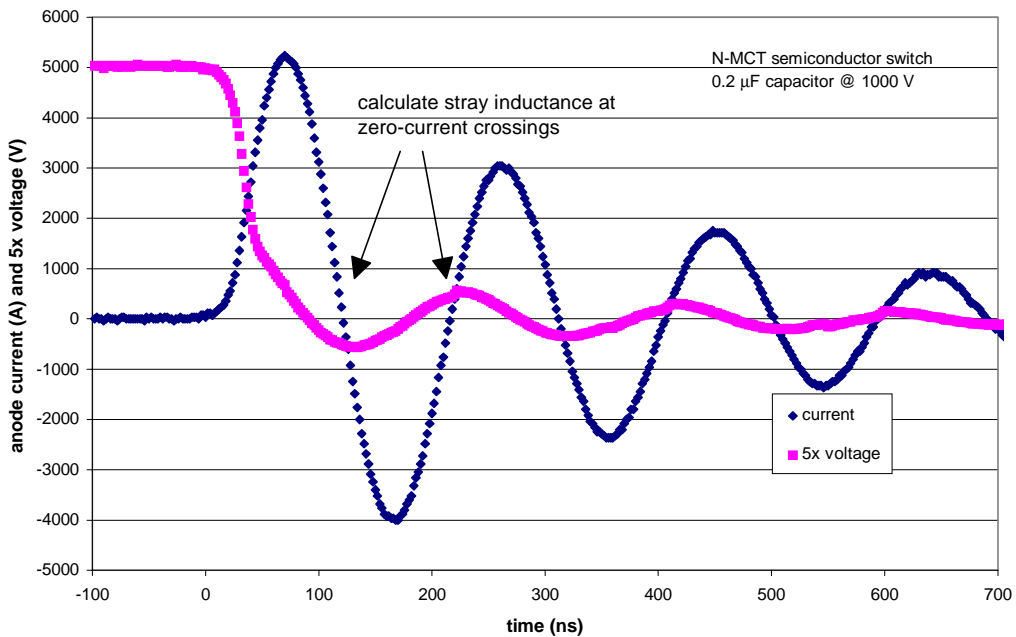


**Figure 3. Voltage and Current Phase Shift.** If the voltage across the switch includes appreciable stray inductance, there is a noticeable phase shift between the current and voltage waveforms. In this example, the stray inductance amounted to 0.7 nH. The voltage at a zero-current crossing equals the product of  $dI/dt$  and stray inductance.

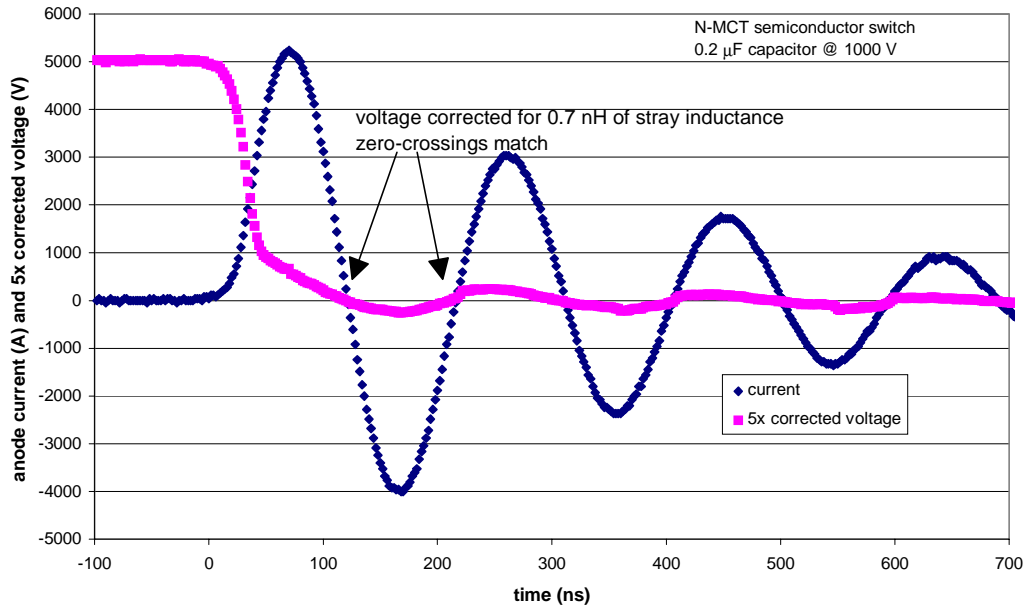


**Figure 4. Voltage Corrected for Stray Inductance.** The voltage waveform can be corrected for stray inductance by subtracting the product of stray inductance and  $di/dt$ . The corrected voltage is now in phase with the current waveform and represents the voltage drop due to switch resistance.

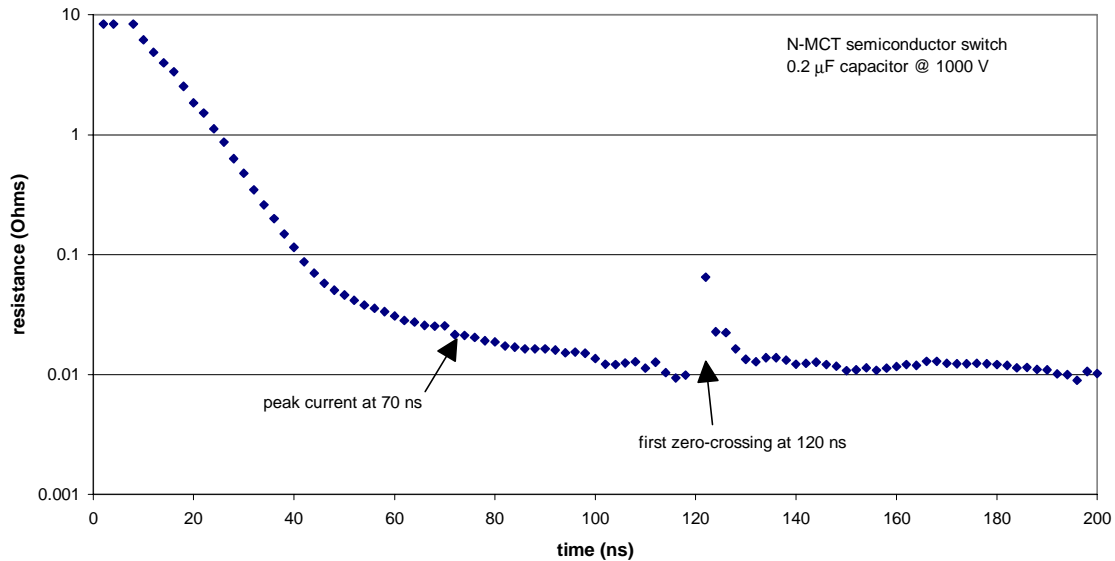


**Figure 5. Switch Turn-On Resistance.** The resistance of the switch is calculated by dividing the corrected voltage by the current. Near zero current, the resistance is poorly determined and dominated by noise in the current waveform.

# Gas Switches

Conceptually, a gas switch is a very simple device. Two electrodes, an anode and a cathode, are separated by a gap composed of neutral gas molecules or atoms. Initially, the gap is an excellent insulator. When the electrodes are biased at a large voltage, the electric field in the gap is large; and if a stimulus generates enough free electrons, it triggers an electron avalanche that rapidly transforms the neutral gas into electrically conductive plasma. A large amount of research on electron avalanche in gases has been done,<sup>2</sup> but published work on the practical aspects of designing gas switches for fuze applications is limited. One good reference is a report by Williams<sup>3</sup> on the detailed design of triggered spark gaps.

The earliest gas switches were two-terminal open-air gaps that were triggered by increasing the voltage until breakdown occurred. As an example, Heinrich R. Hertz, the first to demonstrate radio waves in 1888, used open-air spark-gap switches in his pioneering experiments. To be practical for fuze applications, the switch must operate in a variety of environments, and it must activate at a precise time on command. In lieu of the early two-terminal open-air gap, the typical gas switch of today is a three-terminal device (anode, cathode, and trigger) with the gas sealed inside a hermetic envelope. Figure 6 shows a generic triggered gas switch tube. A high-voltage trigger pulse breaks down the small gap between the trigger pin and the adjacent electrode, and in turn, the free electrons generated by the trigger pulse cause the main anode-cathode gap to break down.

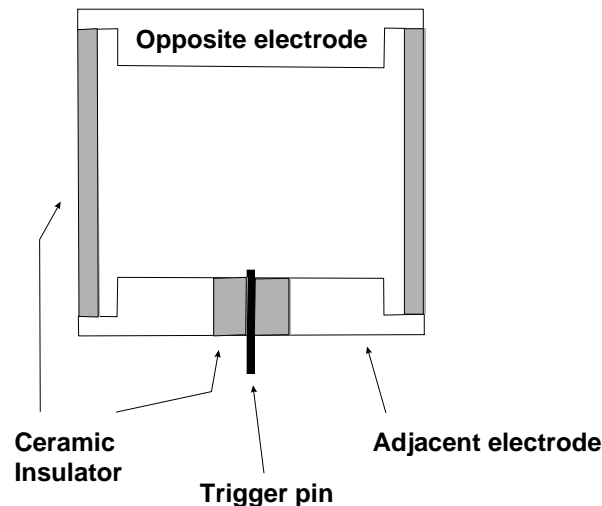


**Figure 6. Gas Switch.** The typical gas switch is a sealed three-terminal device that is filled with gas. A high-voltage pulse between the trigger pin and the adjacent electrode initiates switch turn-on. The gas switch can operate in one of four modes defined by the polarity of the trigger relative to the adjacent electrode and the polarity of the opposite electrode relative to the adjacent electrode.

Much of the scientific literature on the electrical breakdown of gas gaps is not directly relevant to the design of gas switches. In a typical investigation, the electrodes are frequently reconditioned to prevent electrode-erosion effects from confounding the experiment. Furthermore, the gas is continuously replenished and maintained at constant pressure. This environment provides stable conditions for studying gas gap breakdown, but it does not provide a good simulation of a permanently sealed gas switch. Many irreversible changes occur that limit the operating life of a sealed gas switch. For example, some interactions scavenge the gas, leading to lower static-breakdown voltages. On the other hand, opposing processes, such as heat, may release gas. In addition, the electric arc erodes the electrodes and sputters the metal throughout the tube. The sealed gas switch tube is a dynamic device whose characteristics are changing as the switch fires. Some parameters change in a predictable manner, but other changes are chaotic and less predictable.

Paschen's law states that the breakdown voltage of a gas gap is invariant if the product of the gas pressure and the gap spacing is constant (denoted by  $pd$  where  $p$  = pressure and  $d$  = gap spacing). The breakdown voltage of a gas gap is characterized by the Paschen curve that plots breakdown voltage versus the product of gas pressure and gap spacing (see Figure 7). A gas switch is to the right of the Paschen minimum. For small values of  $pd$  well to the left of the Paschen minimum (the regime of vacuum switches), Paschen's law is no longer applicable.<sup>4</sup> At very low pressures, the breakdown voltage of the gap is independent of gas pressure and is determined by gap spacing, electrode-surface finish, electrode material, etc. When contaminants are present (e.g., inclusions of foreign material in the electrode), the electric arc may release small amounts of gas. In a gas switch, this is inconsequential. The additional amount of gas is small compared to the original amount of gas, and the additional gas only drives the switch away from the Paschen minimum. In a vacuum switch, the released gas will be more noticeable. Measured as a fraction of gas originally present, the amount of released gas may be large. The most serious consequence is a lower breakdown voltage because a gas release drives a vacuum switch toward the Paschen minimum. For these reasons, the design and fabrication of a good vacuum switch is technically more challenging than that of a gas switch. Purity of materials and contamination of parts are problems that have more serious consequences in a vacuum switch than in a gas switch.

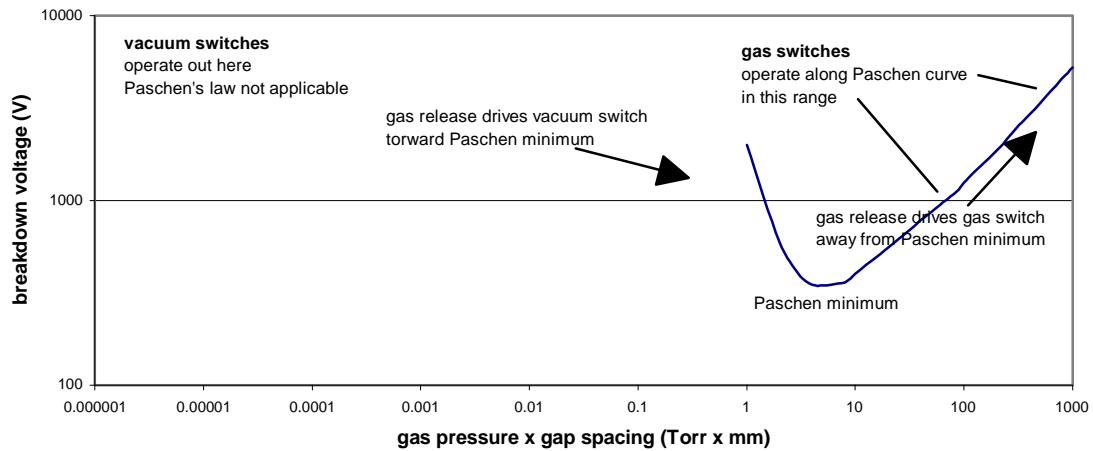


**Figure 7. Relationship of Gas and Vacuum Switches.** Gas switches operate on a Paschen curve to the high-pressure side of the Paschen minimum. Vacuum switches operate at very low pressures where Paschen's law is not applicable. If trapped gas is released, a vacuum switch is driven toward the Paschen minimum, but a gas switch is driven away. If gas is removed by the scavenging action of the electric arc, the static-breakdown voltage of a gas switch decreases.

## First-Shot Effect

The static-breakdown voltage (SBV) is a critical parameter for any gas switch tube. If the current pulse passing through the gap is small, the SBV of a well-designed gap remains constant to within a few percent for many thousands of breakdown cycles. Figure 8 shows 500 SBV measurements of a low-cost gas gap (CG3-1.5L rated at 1.5 kV breakdown and manufactured by CP Clare). Except for the first shot, all measurements were repeatable to within 2%. In this test, we applied an increasing voltage (about 4 V/s) across the gas gap and a 180 pF capacitor. When the voltage ramp reached breakdown, the gap suddenly discharged the capacitor, generating a small current pulse (6 A peak current and 100 ns long). The gap broke down about once per minute during this test. If the energy of the arc is sufficiently small, the gas gap will suffer no appreciable damage, and the SBV will be stable.

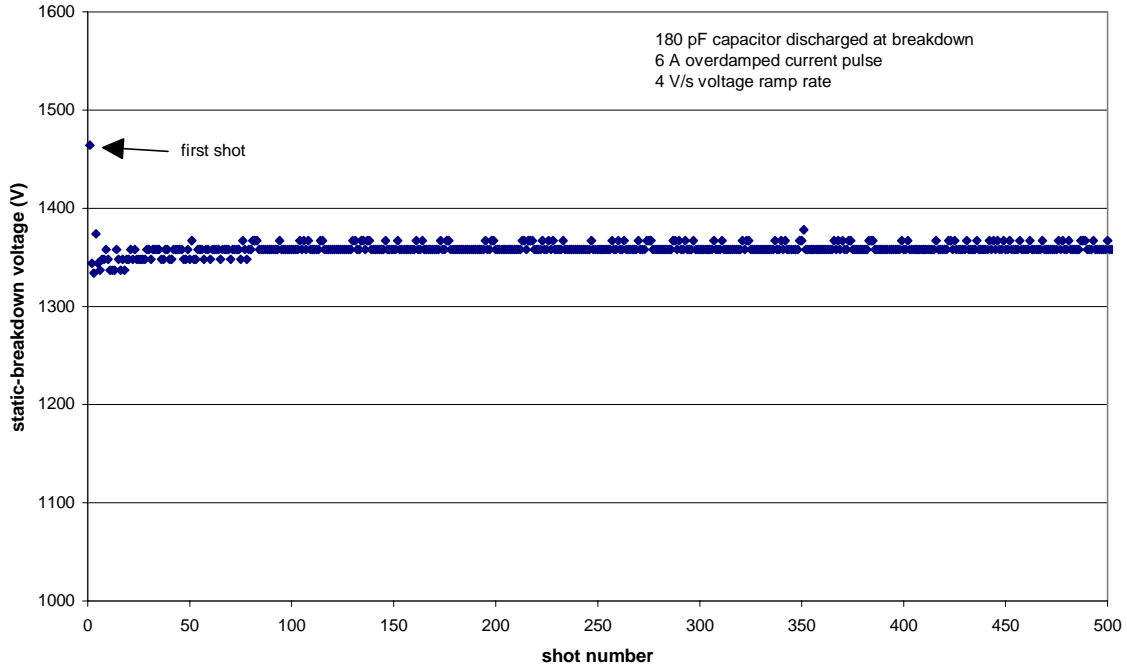


**Figure 8. SBV Stability at Low-Current Pulse.** At low-current pulse, the static-breakdown voltage of a gas gap may be very stable (a few percent) over thousands of cycles. In this example, the gas gap discharged a 180 pF capacitor at breakdown, producing a peak current of 6 A. The voltage ramp was very slow, about 4 V/s.

After an extended period of inactivity, the first breakdown voltage is often higher than subsequent breakdown voltages that are separated by minutes. The precise underlying physical mechanisms of this “first-shot effect” are not well understood. Some manufacturers place a radioactive element inside their gas gaps to reduce the first-shot effect and to help stabilize the SBV. In many cases, the first-shot effect is not detrimental because it improves immunity against hold-off failures. Possible exceptions include applications where accurate timing is crucial. To investigate the magnitude and the prevalence of the first-shot effect, we made 50 SBV measurements for each of 20 new CG3-1.5L gas gaps. In Figure 9, we plot the SBV of the first shot and the average of 50 repeated SBV measurements. In 18 out of 20 gaps, the highest SBV corresponded to the first shot, but the magnitude of the first-shot effect varied from negligible to 40%; that is, the first-shot SBV was 40% larger than the average SBV.

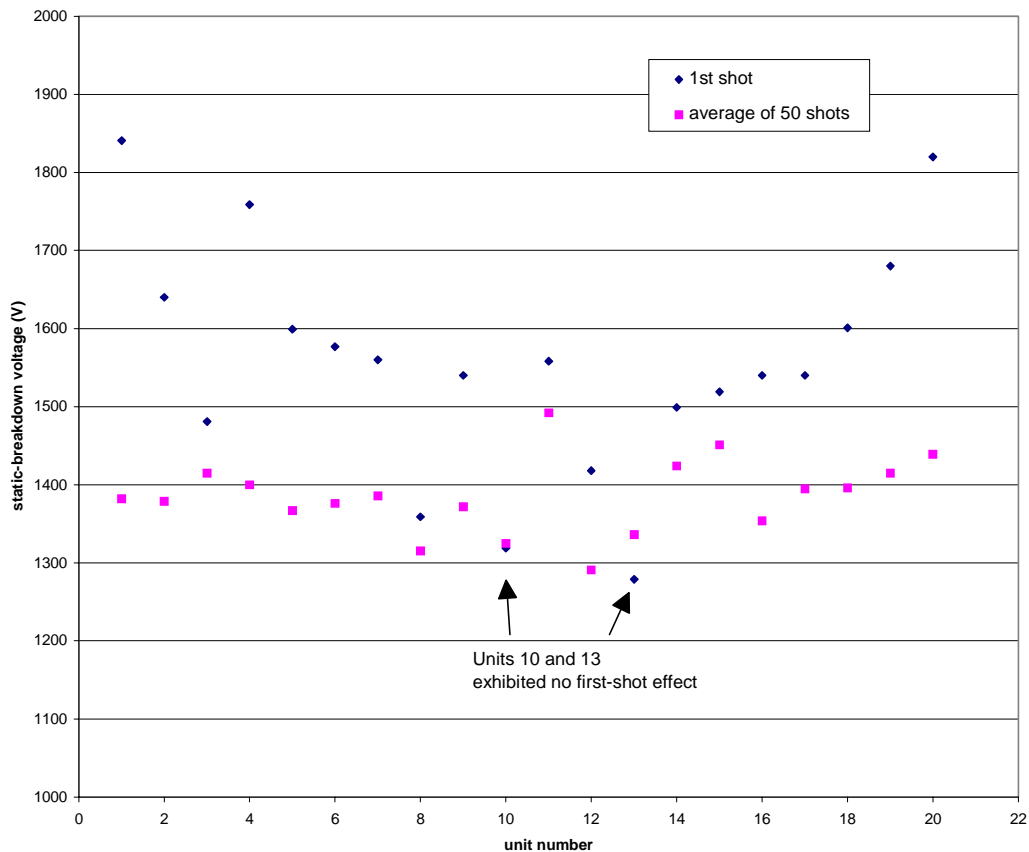


**Figure 9. First-Shot Effect in a Gas Overvoltage Gap.** In 18 out of 20 gaps, the highest SBV (in a run of 50 measurements) corresponded to the first shot. In some units this first-shot effect was substantial, but in others it was insignificant. Units 10 and 13 did not exhibit a first-shot effect. The gaps were CG3-1.5L gas gaps made by CP Clare with a nominal 1.5 kV breakdown voltage.

## Degradation of the SBV

At current levels of thousands of amperes, the electric arc significantly alters the SBV. In some switches, a small amount of gas is removed with each shot, and the SBV decreases as the number of shots increases. We monitored the SBV degradation of two CG3-1.5L gas gaps fired in two different capacitor-discharge circuits: the first was a 0.2  $\mu\text{F}$  over-damped circuit producing a 2 kA nonringing current pulse, and the second was a 0.4  $\mu\text{F}$  under-damped circuit producing a 6 kA ringing current pulse. On a per-shot basis, the total charge passing through the gap in the 0.4  $\mu\text{F}$  circuit is about 12 times greater than in the 0.2  $\mu\text{F}$  circuit. To compare SBV degradation in the two circuits, we plotted SBV versus the accumulated charge flow as opposed to SBV versus the number of shots. The results are shown in Figure 10. For the same amount of accumulative charge flow, the SBV deteriorates more rapidly with fewer shots at higher currents than more shots at lower current.

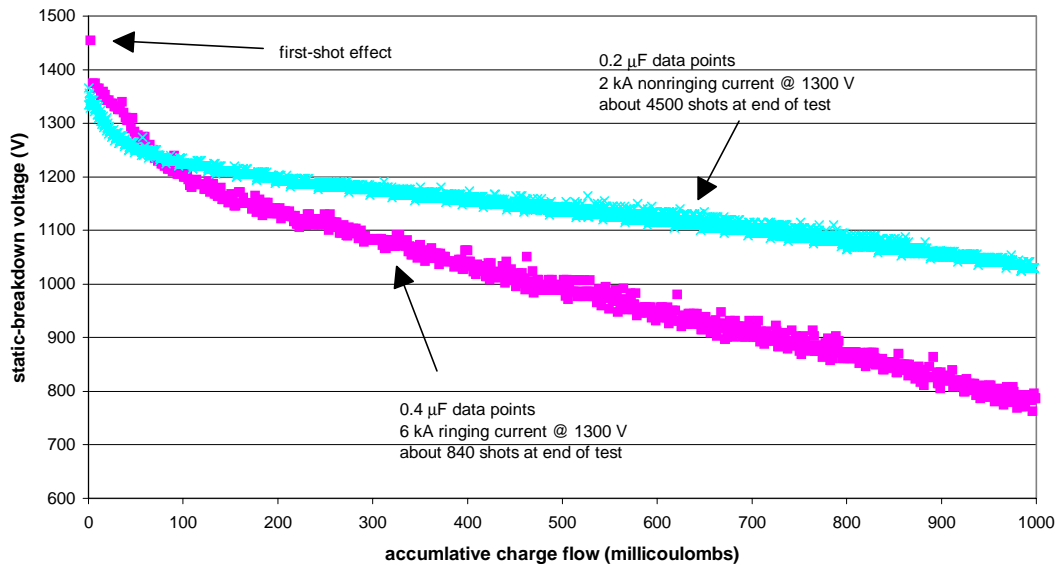


**Figure 10. SBV Degradation at High-Current Pulse.** With peak currents in the kiloampere range, the SBV of the gas gap decreases as a result of the gas-removal action of the electric arc. One gap discharged a 0.4  $\mu\text{F}$  capacitor in an underdamped circuit (ringing current of 6 kA at 1300 V). The other gap discharged a 0.2  $\mu\text{F}$  capacitor in an overdamped circuit (nonringing current of 2 kA at 1300 V). For a single shot at the same voltage, the total charge passing through the gap in the 0.4  $\mu\text{F}$  circuit was about 12 times greater than in the 0.2  $\mu\text{F}$  circuit.

The degradation of the SBV depends on the type of gas inside the tube. Using the same test circuit, we fired two triggered spark gaps (GP-466 manufactured by EG&G): one filled with nitrogen and the other filled with xenon. In both cases, the peak current was in the 8 kA to 9 kA range, and the circuit was underdamped, producing a ringing waveform. Figure 11 shows the SBV for the first 1200 shots. The SBV of the nitrogen-filled switch decreased steadily. The SBV of the xenon-filled switch did not decrease, but it did become more erratic. Xenon is an inert noble gas and, in comparison to nitrogen, is less readily removed by the electric arc.

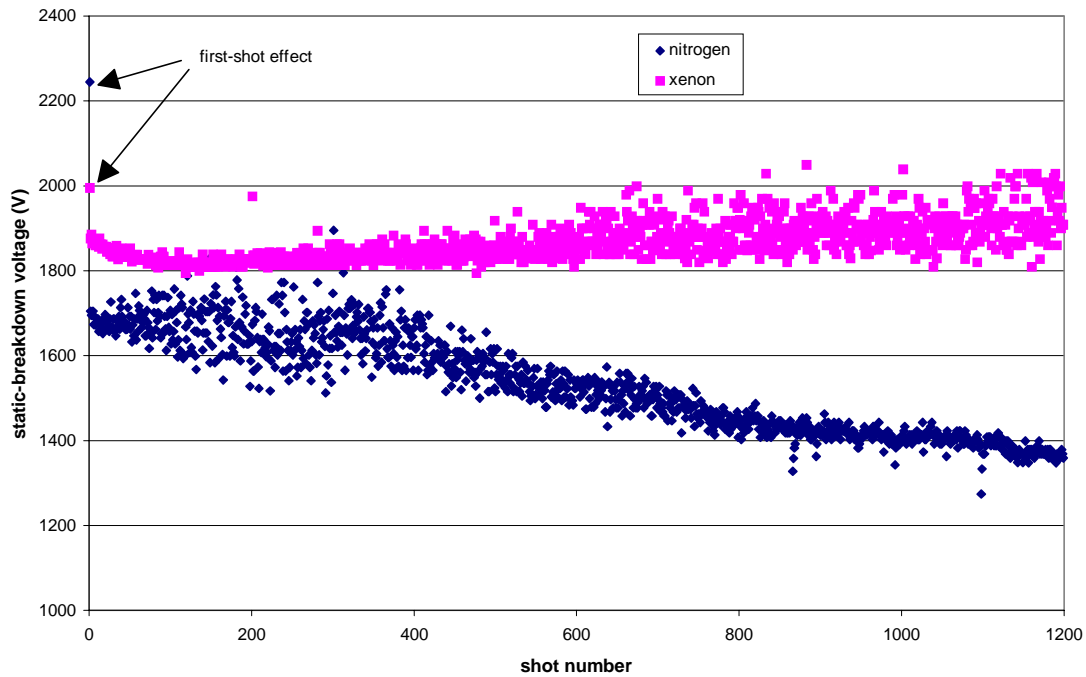


**Figure 11. SBV Degradation and Gas Fill.** The gas fill affects the SBV of a gas switch subjected to repeated discharges. In this example, a nitrogen-filled switch and a xenon-filled switch discharged a 0.4  $\mu\text{F}$  capacitor, producing an 8 kA to 9 kA peak current. The SBV of the nitrogen switch steadily decreased, but the SBV of the xenon tube remained nearly constant.

The degradation of the SBV is often more erratic than shown in Figure 10. In place of a smoothly decreasing function, there may be discontinuities where the SBV suddenly drops. The most disturbing event is the single isolated shot with sharply lower SBV among other data points that otherwise indicate a slowly decreasing SBV. In Figure 12 we show the SBV of a 3 kV gap (CG3-3.0L made by CP Clare) discharging a 0.4  $\mu\text{F}$  capacitor at 15 kA peak current. These isolated SBV anomalies are troublesome because they would cause a hold-off failure if the SBV dropped below the operating voltage.

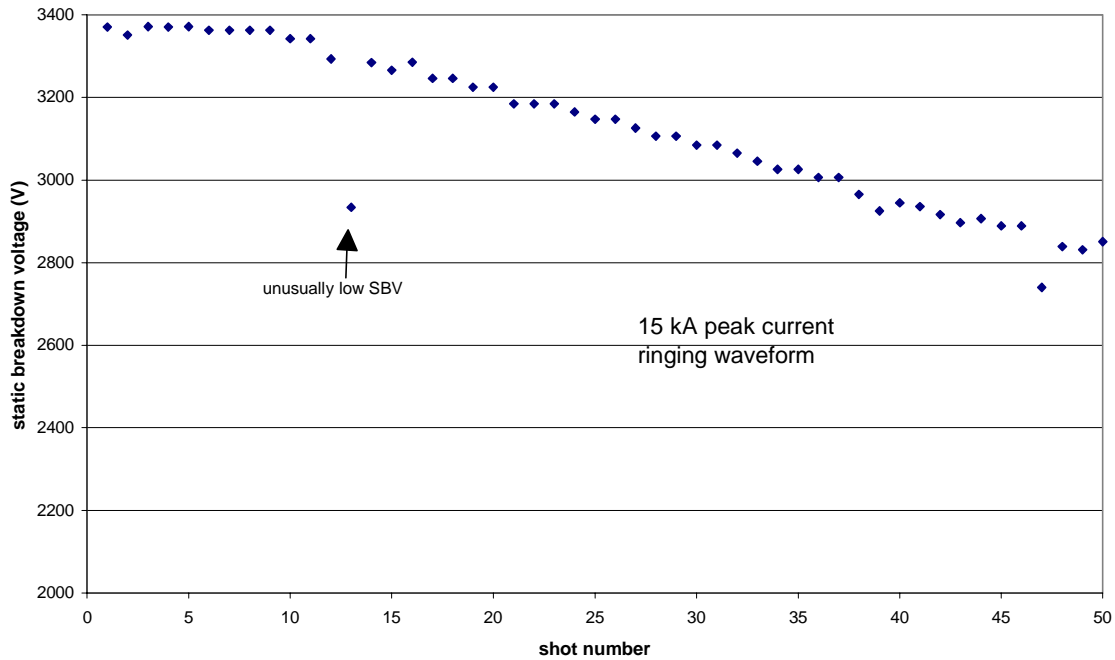


**Figure 12. Isolated-SBV Anomaly.** Rather than exhibiting a smooth gradual decrease, the SBV may drop very suddenly. A CP Clare overvoltage gap discharged a 0.4  $\mu\text{F}$  capacitor, producing a 15 kA peak current. On shot 13, the SBV dropped well below nearby shots.

The scavenging of gas is reversible to a limited extent. The trapped gas is partially released by heating the switch to a high temperature. To illustrate this and the first-shot effect, we measured the SBV of a CG3-1.5L gap as before except that we interrupted the normal test sequence to either heat the gap or to let the gap remain idle for an extended period of time. The results are shown in Figure 13 where heating and idleness appreciably altered the SBV. The first-shot effect is probably related to gases adsorbed on the surface of the electrodes that are released after a single shot. Conversely, heating the switch releases enough gas that it takes several shots for this gas to be removed.

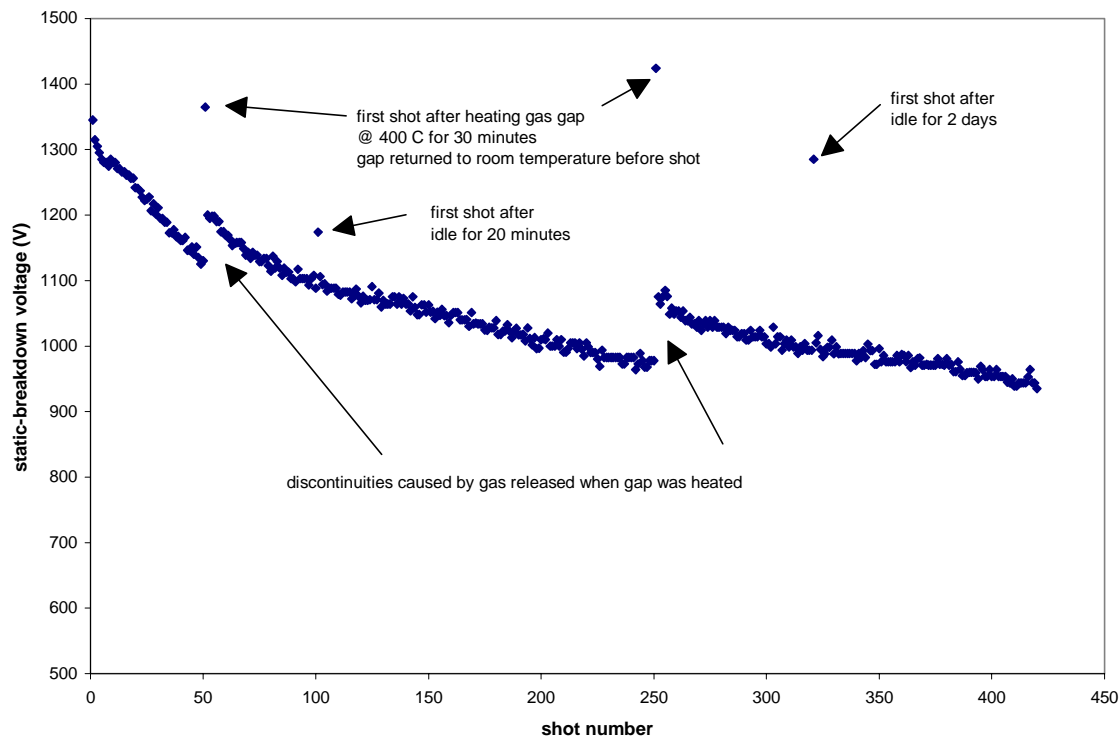


**Figure 13. Gas Release by Heating.** The steady decline of the SBV caused by gas removal can be partially reversed by heating the switch and releasing gas. We interrupted the normal test sequence after shots 50 and 250 to heat the gap. After the gap cooled back to room temperature, we resumed the SBV test. The heating produced discontinuities in the otherwise steadily decreasing SBV. The first-shot effect is also apparent, but it alters the SBV for only a single shot.

## Operating Voltage Range

The voltage range of a gas switch is much more limited than the voltage range of a vacuum switch. The SBV is an absolute upper limit; and in practice, gas switches operate no higher than 80 to 90 percent of the SBV. Three considerations determine the maximum operating voltage: (1) allowance for unit-to-unit variations of SBV, (2) allowance for SBV degradation over the required shot life, and (3) reliability against hold-off failure. At the other extreme, timing jitter and reliability against no-fire failures dictate the lowest operating voltage. Timing jitter rapidly increases as the operating voltage drops below 50% of the SBV, and eventually no-fire failures occur.

To illustrate the relationship between timing jitter and operating voltage, we fired a gas switch 270 times as the voltage repeatedly cycled from 700 V (40% of SBV) through 1500 V (86% of SBV) in 100 V increments. The corresponding peak current varied from 1900 A to 4800 A. Figure 14 is a scatter diagram of the trigger-break to the anode-current delay at the nine operating voltages. Below 1000 V (57% of SBV), the scatter of TAD2 increases rapidly. However, from a systems perspective, the relevant delay is the start of trigger to anode-current delay, and if it is plotted in the same fashion (see Figure 15), the increased timing jitter at lower voltages is not nearly as dramatic. The cause becomes

clearer if we plot the trigger-break voltage versus operating voltage, as shown in Figure 16. Note that the large scatter of trigger-break voltage tends to dominate TAD. The cause for this high variability is not known.

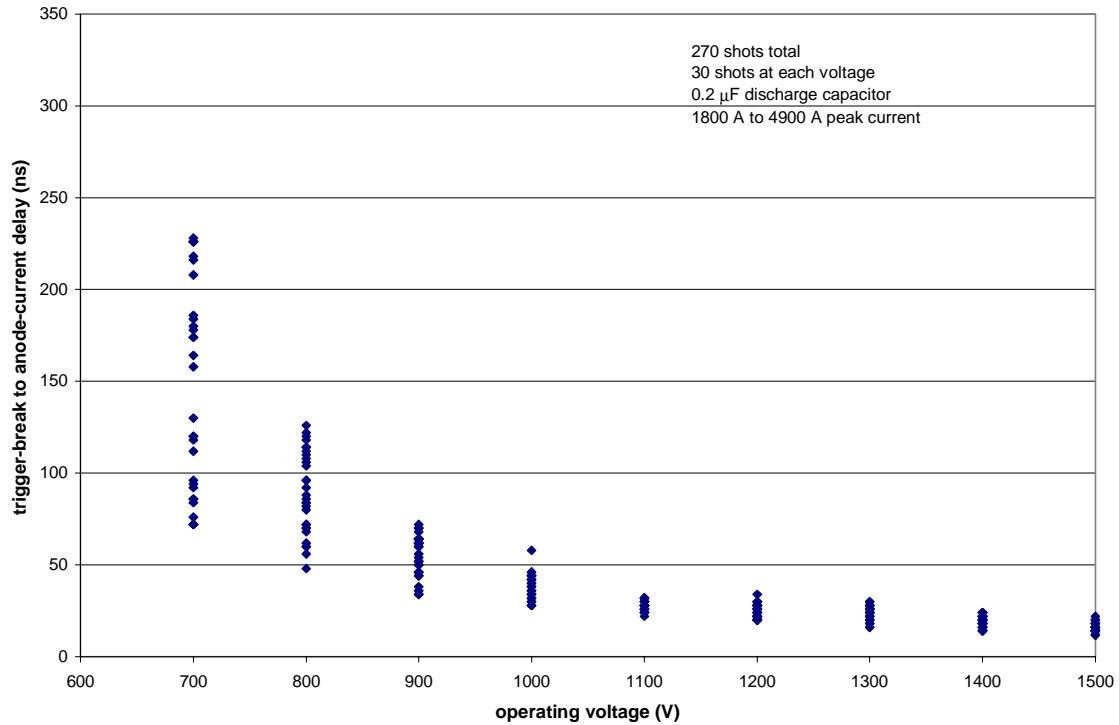


**Figure 14. TAD2 and Operating Voltage.** The instability of TAD2 increases substantially as the operating voltage drops below 50% of the SBV. The test switch was a GP466 triggered gas switch made by EG&G with an 1800 V SBV when new.

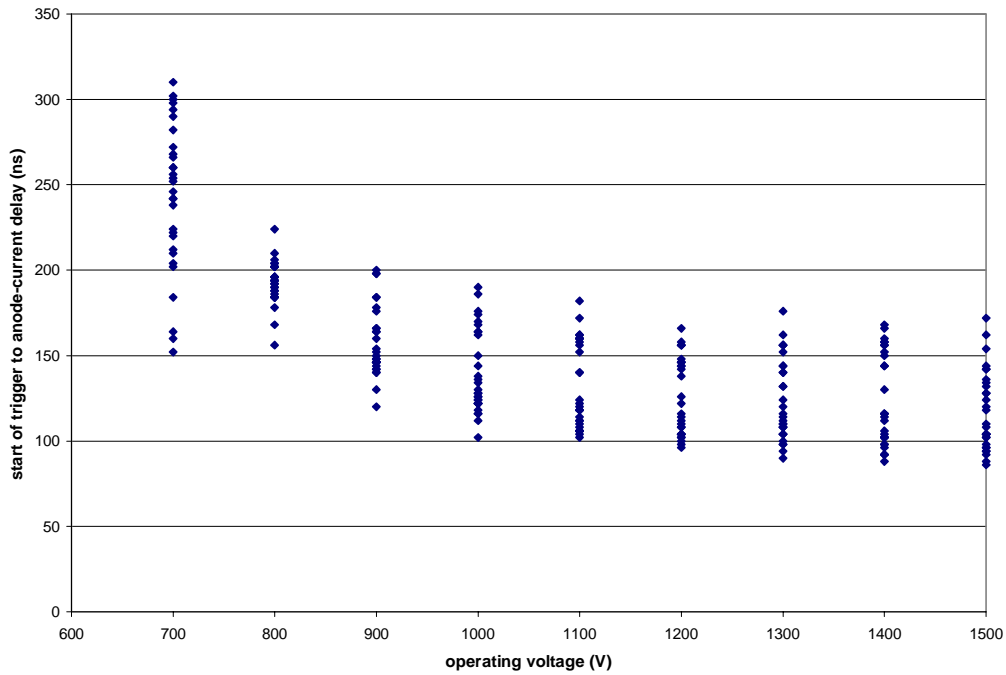


**Figure 15. TAD and Operating Voltage.** In contrast to TAD2, the scatter of TAD is nearly independent of operating voltage. Except for 700 V, the variance of TAD is more dependent on a highly variable trigger-break voltage than on the variability of TAD2.

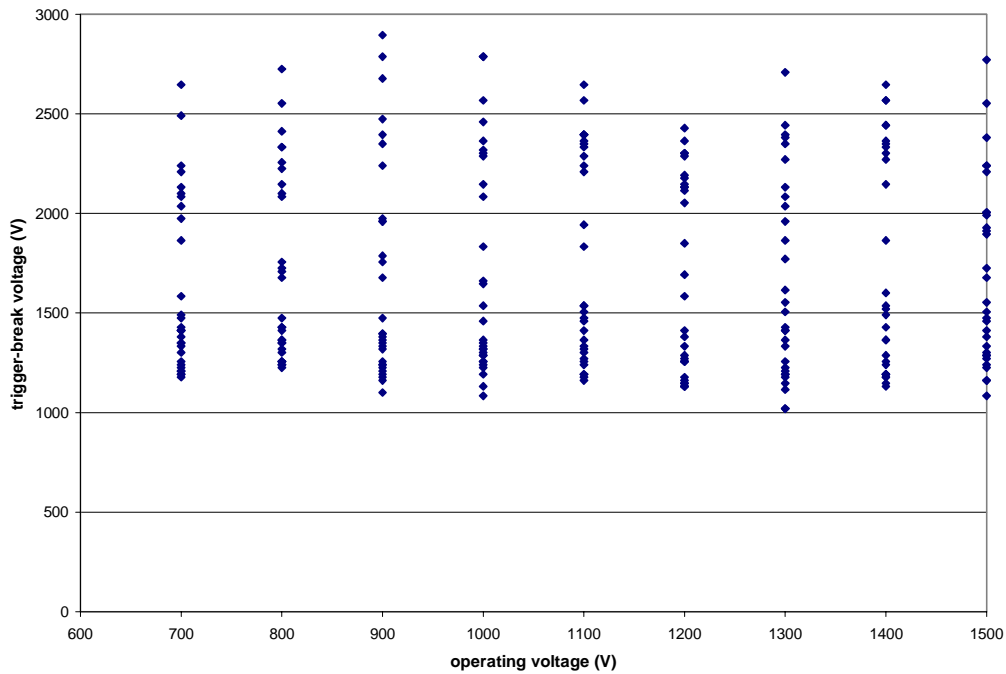


**Figure 16. Trigger-Break Variability.** The trigger-break voltage had a large amount of scatter independent of the operating voltage, roughly 1000 V to 2500 V. With a trigger-ramp rate of 15 V/ns, the variable trigger-break voltage will contribute 100 ns of timing jitter.

## Triggering Mode

Gas switches can operate in four modes that are determined by the polarity of the trigger with respect to the adjacent electrode and the polarity of the adjacent electrode with respect to the opposite electrode. We took a GP466 nitrogen switch and fired it in all four modes, taking twenty shots in each mode for a total of 80 shots. The most distinctive difference between the modes is provided by TAD2 (see Figure 17). The two modes in which the trigger pin is driven in a polarity counter to the opposite electrode produce the shortest TAD2. However, the total delay, TAD, is nearly 10 times larger than TAD2; and the erratic trigger-break voltage dominated the TAD variability. Thus, the TAD jitter is nearly independent of operating mode (see Figure 18).

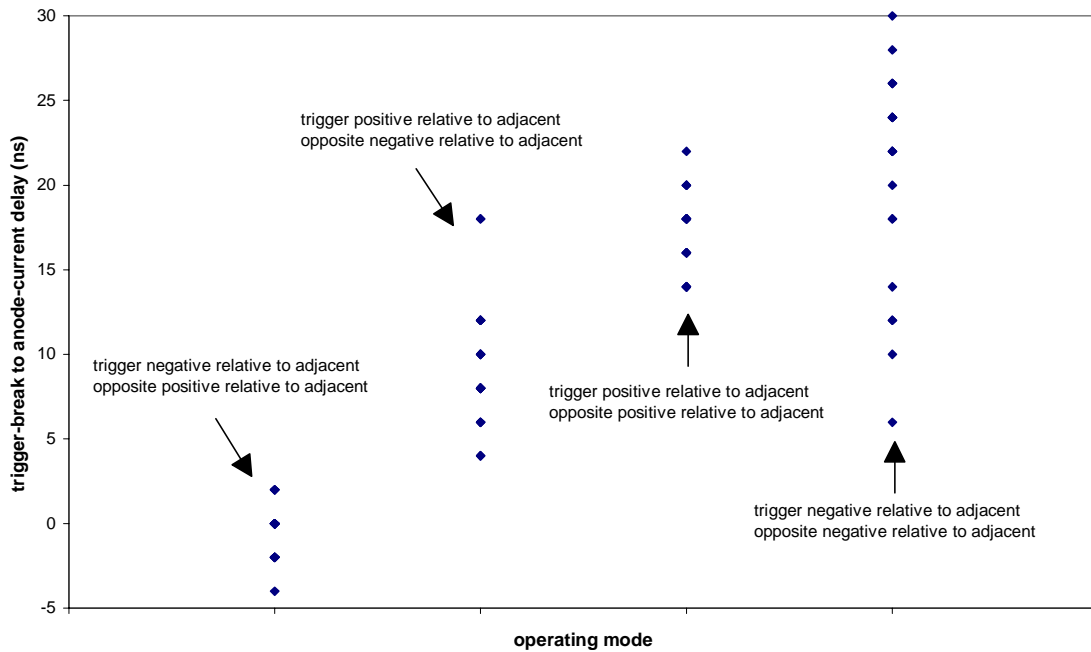


**Figure 17. TAD2 and Operating Mode.** TAD2 is dependent on the operating mode. In this test, there were twenty shots at each mode. The switch was a nitrogen-filled tube with an SBV of 1800 V. The switch operated at 1400 V discharging a 0.2  $\mu\text{F}$  capacitor, producing a 4.6 kA peak current.

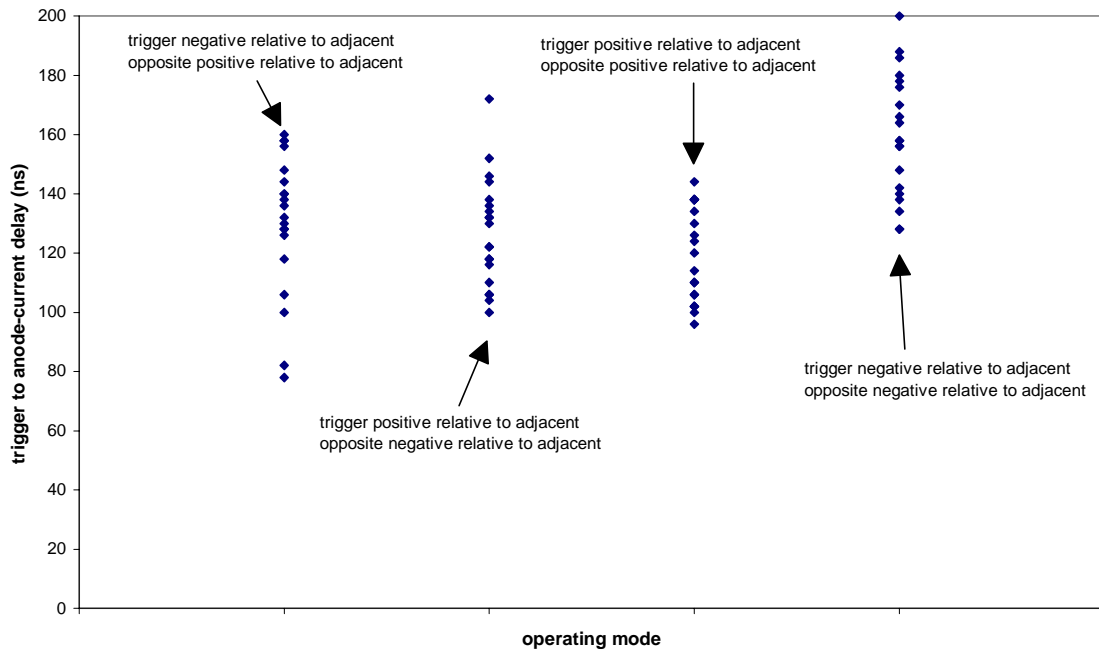


**Figure 18. TAD and Operating Mode.** The TAD variance is nearly independent of the operating mode. The variability of the trigger-break voltage effects TAD more than the variability of TAD2. This data comes from the same test as in Figure 17.

## Switch Aging

Besides the decline of the SBV, gas switches may exhibit other aging effects. In Figure 19, TAD and TAD2 are plotted against shot number for the first 500 shots of a nitrogen-filled switch. Note that TAD2 is relatively stable, but TAD shifts from 210 ns to 150 ns at about shot 150. The decrease in TAD is associated with a decrease of the trigger-break. Also note that the timing jitter decreases past shot 200. It is common for gas and vacuum switches to exhibit various sorts of aging behavior. In some cases, a switch may be intentionally fired some number of shots at the factory in an effort to improve switch performance.

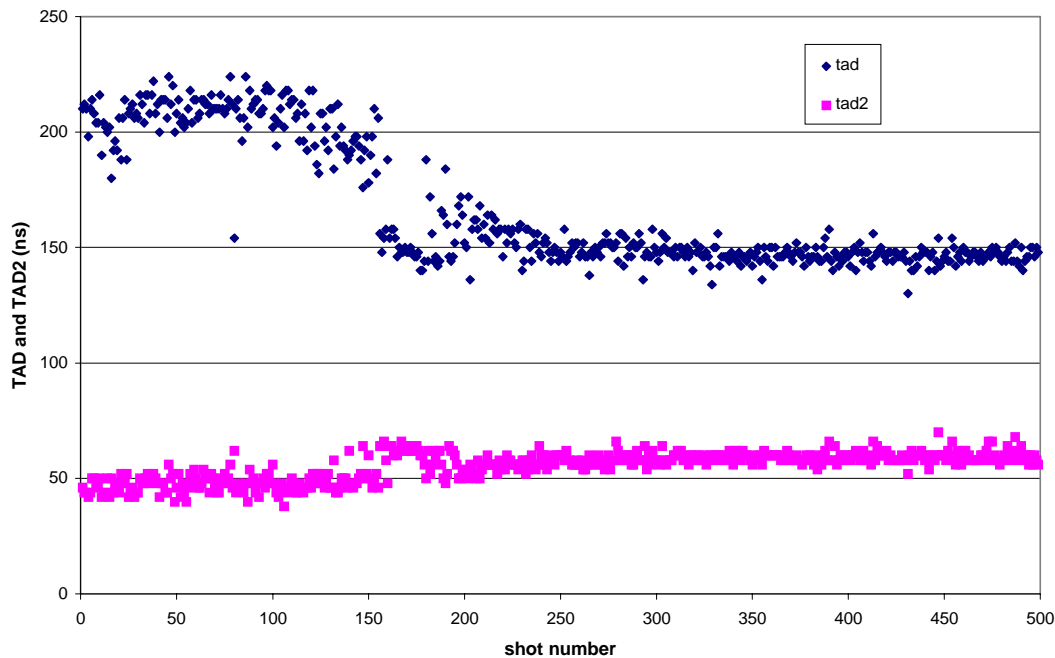


**Figure 19. Aging of a Gas Switch.** As a gas switch operates, the electric arc irreversibly alters the switch with each shot, and the switch changes as more shots accumulate. In this example, a new nitrogen-filled switch discharged a 0.2  $\mu\text{F}$  capacitor at 1000 V, producing a 3 kA peak current. The TAD suddenly decreased around shot 150 when the trigger-break voltage dropped.

## Hybrid Switch

Most gas switches are three-terminal devices, but a low-cost two-terminal over-voltage gap can also function as a switch. We developed a method to overvoltage a gas gap using a diode—hence the name *hybrid* (gas and semiconductor [see Figure 20]). The hybrid switch preserved the timing accuracy of a three-terminal gas switch, and it also consisted of two low-cost parts (a few dollars): a two-terminal gas gap and a diode. The basic idea is that the trigger voltage initially places the diode under reverse bias. The polarities are such that the trigger voltage and the main capacitor voltage are additive, and their sum appears across the gas gap. At some point, the gas gap breaks down, and the diode suddenly becomes forward-biased by the main capacitor, resulting in a large current pulse. The disadvantage of the hybrid switch is that the main discharge current must pass through a gas gap and a diode, thereby increasing resistance and inductance. Consequently, the performance of the hybrid switch suffers in comparison to other gas switches. Nevertheless, the hybrid switch can provide stable performance over many hundreds of shots with low timing jitter (see Figure 21).

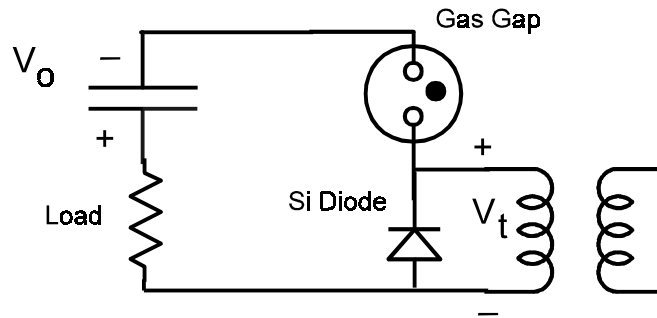


**Figure 20. Hybrid Switch.** The hybrid switch consists of a gas overvoltage gap and a diode. Prior to the trigger pulse, the gap holds off the main capacitor bias voltage,  $V_0$ . As the trigger-pulse voltage increases, the voltage across the gap increases, equaling  $V_0 + V_t$ . Eventually the gas gap suffers electrical breakdown and places the diode under forward bias, discharging the main capacitor.

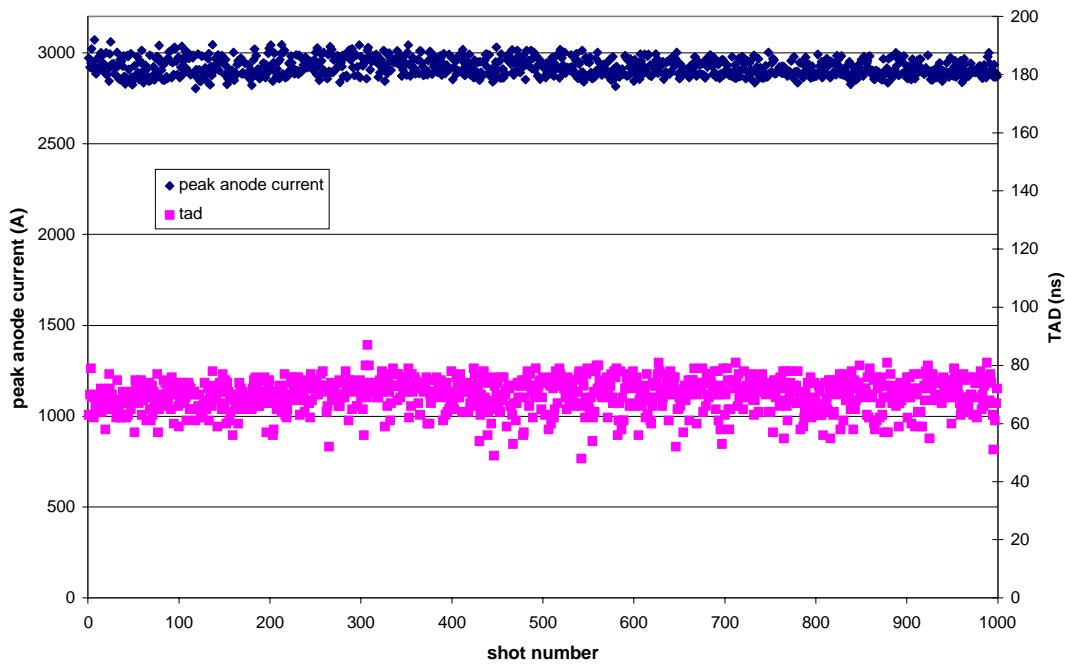


**Figure 21. Hybrid Switch Pulse-Life Test.** This hybrid switch consisted of a low-cost transient suppressor (CG3-1.5L from CP Clare) and a low-cost diode (MR760 from Motorola). The switch operated in a low-impedance discharge circuit with a  $0.2 \mu\text{F}$  capacitor charged to 1000 V.

# Vacuum Switches

In vacuum switches, the gas pressure is so low that the mean-free path of an electron greatly exceeds the anode-cathode separation, precluding electron avalanche in the residual gas. In a high-quality vacuum switch, the amount of residual gas is too small to affect switch behavior throughout the design-life of the switch. Not only must the initial vacuum be good, but there also must be no significant gas release under the stimulus of the electric arc. High-quality vacuum is not easily achieved and requires careful material selection and meticulous assembly techniques.<sup>6</sup> In some cases, commercially available vacuum switches fall short and contain significant amounts of residual gas. The amount of gas in these switches will change, depending on the balance between gas-release and gas-scavenging processes. Excessive residual gas is most readily detected by looking for TAD changes in response to temperature variations.

The structure of a vacuum switch (see Figure 22) is very similar to that of a gas switch except for the trigger mechanism. In a gas switch, a high-voltage trigger pulse breaks down the small gas gap between the trigger pin and the adjacent electrode. In most vacuum switches, a carbon film connects the trigger pin and the adjacent electrode, replacing the gas gap. The trigger pulse produces surface breakdown on the carbon film, generating a small amount of plasma. Eventually, the plasma fills the main cathode-anode gap and thereby closes the switch. Typically, a wet-carbon process, either hand-painted or sprayed, forms the carbon film. The durability of this carbon film, however, has created reliability problems. Carbon vapor deposition has recently been shown to be a superior technique.<sup>5</sup>

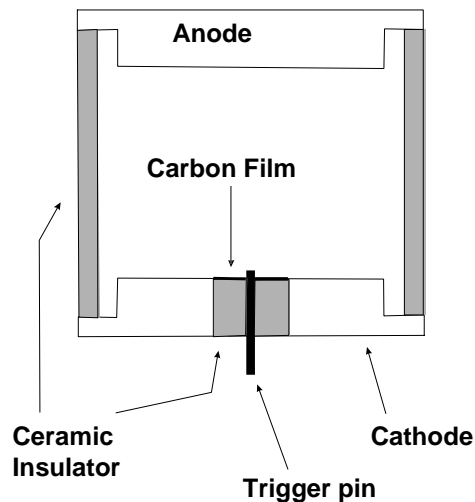


**Figure 22. Vacuum Switch.** This is a diagram of a generic vacuum switch. Most vacuum switches contain carbon film, but some designs avoid carbon. Carbon-free switches are triggered by electrical breakdown across a narrow gap. The adjacent electrode is usually the cathode because less trigger energy is required than if the adjacent electrode were the anode. Despite their name, vacuum switches often contain noticeable amounts of residual gas.

## First-Shot Effect in a Vacuum Switch

Vacuum switches may exhibit a first-shot effect that manifests as an excessively large TAD on the first shot after an extended period of idleness. The underlying mechanism is not certain, but we speculate that residual gas is slowly adsorbed during extended periods of idleness. This adsorption reduces the amount of residual gas and increases the TAD. The electric arc of the first shot releases the adsorbed gas, and the TAD shifts to a lower value that is consistent with more residual gas.

To illustrate the first-shot effect, we fired an experimental vacuum switch (5 kV and 8 kA peak current) and measured the delay of ten-shot runs with various periods of idleness between runs (see Figure 23). The most pronounced first-shot effect was observed on the very first shot. Although the time interval between manufacture of the experimental vacuum switch and this first shot was not precisely known, it was probably a few months. The first-shot effect also resulted in a lower current; but the decrease was modest, perhaps 5 percent. For the switch shown in Figure 23, the first-shot effect could be eliminated by decreasing the anode-cathode spacing or by altering the position of the trigger pin. When a vacuum switch is being evaluated for the first-shot effect, it must not be subjected to high temperatures (e.g., soldering the switch into the test circuit) immediately before the first firing. Heating may release gas, possibly reducing or even eliminating the first-shot effect. In any application where switching delay is a critical specification, the vacuum switch must be tested for a first-shot effect.

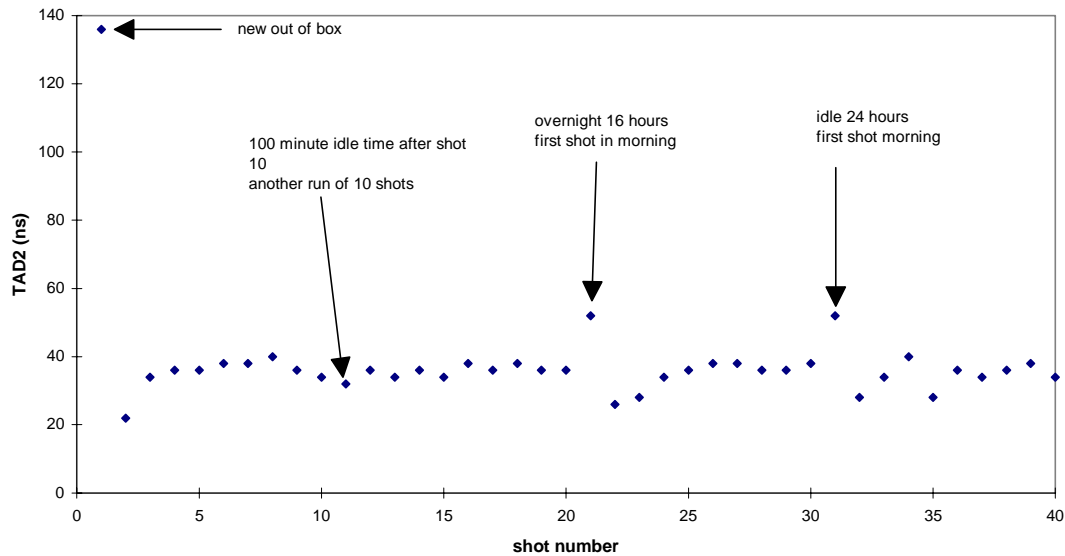


**Figure 23. First-Shot Effect in Vacuum Switches.** In some vacuum switches, a first-shot effect is an excessively long switching delay. We fired the new vacuum switch in a 0.2  $\mu\text{F}$  circuit at 5 kV, producing an 8 kA current pulse. The first-shot effect on shot 1 was quite pronounced. The switch had probably been idle for a few months at this point. After 24 hours, the first-shot effect returned, but the magnitude was modest.

## Low-Temperature and Switch Contamination

If a condensable gas contaminates a vacuum switch tube, the TAD and current may exhibit large perturbations at low temperatures. The TAD of a vacuum switch is normally unaffected by temperature changes (see Figure 24). In a contaminated switch, the TAD at  $-60^{\circ}\text{C}$  is six times longer (see Figure 25), and the peak current is 30% less than at room temperature (see Figure 26). We presume that a contaminant gas, perhaps water vapor, condenses on the carbon-trigger gap at low temperatures and seriously impairs plasma generation.

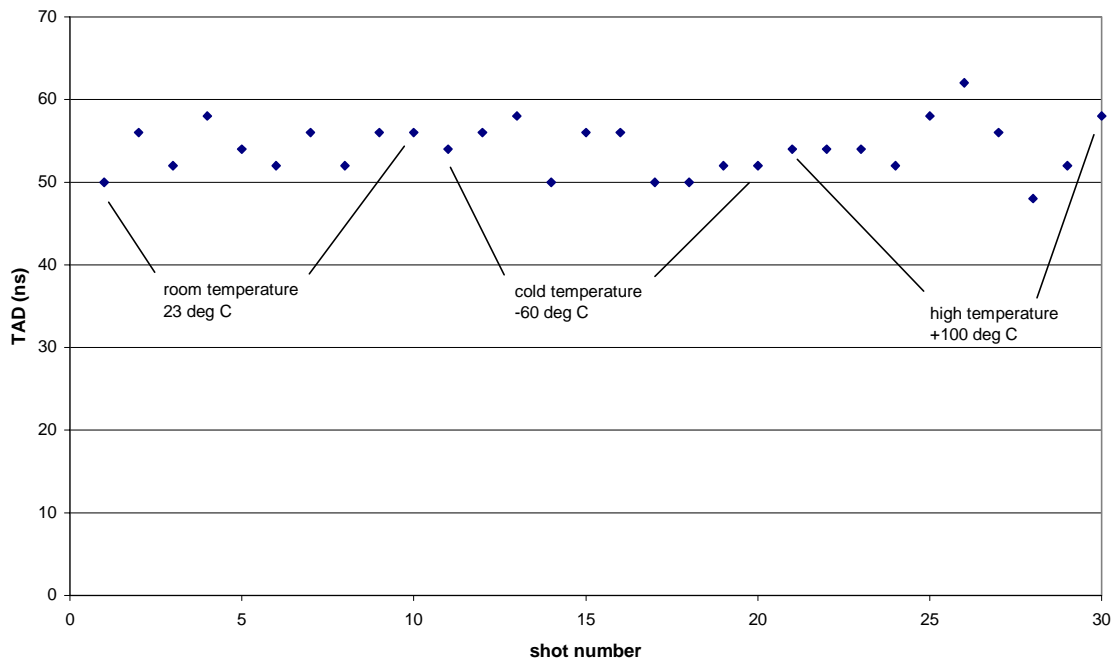


**Figure 24. TAD in Uncontaminated Switch.** The TAD in a high-quality vacuum switch is invariant with respect to temperature. This vacuum switch discharged a  $0.2\ \mu\text{F}$  capacitor, which was charged to 1 kV. From  $-60^{\circ}\text{C}$  to  $+100^{\circ}\text{C}$ , there was no discernible change in the TAD.

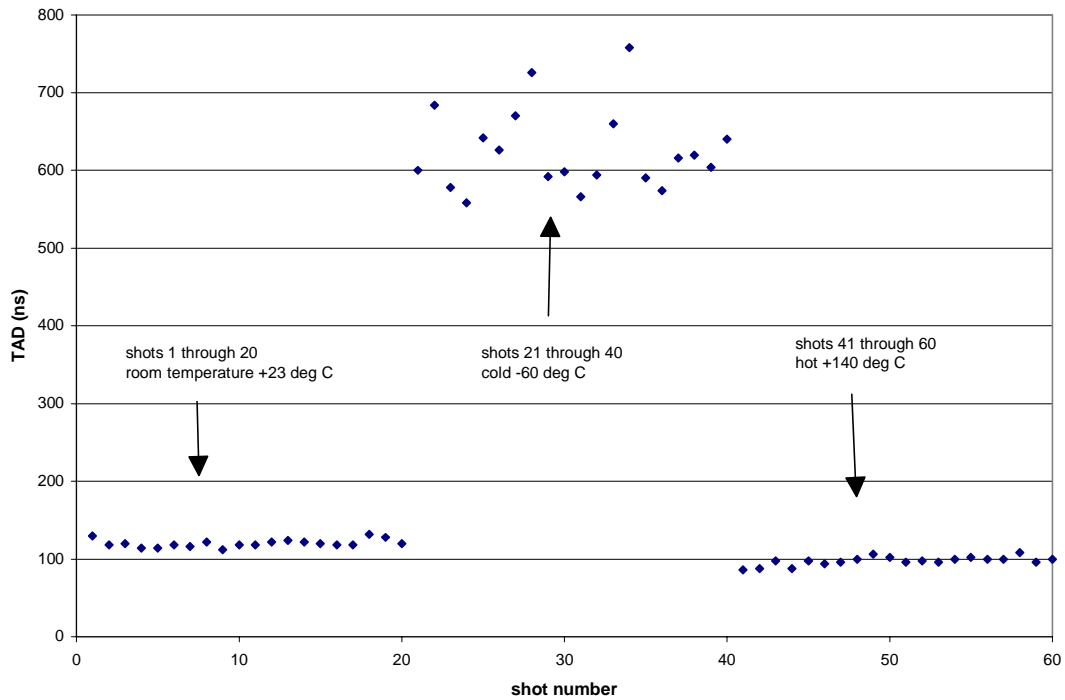


**Figure 25. TAD in Contaminated Switch.** The TAD in a contaminated vacuum switch may exhibit large perturbations at low temperature. In this case, we suspect that a gas that condenses at low temperatures contaminates the switch.

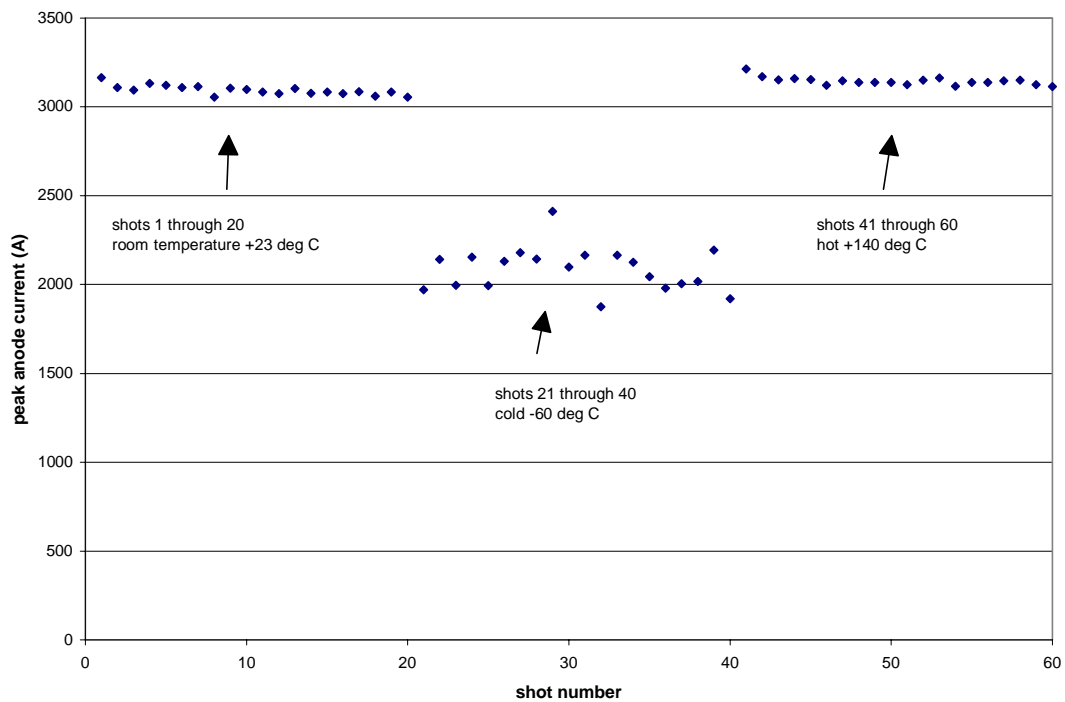
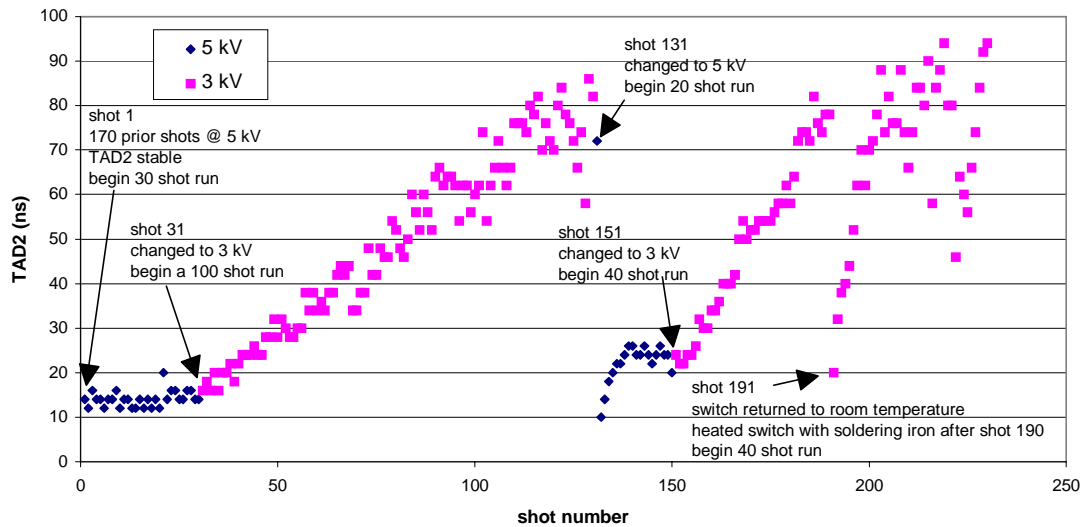


**Figure 26. Peak Current in Contaminated Switch.** The peak current is also vulnerable to large perturbations in a contaminated switch. From the same test as Figure 25, this vacuum switch suffered a 30% decrease of current at low temperature.

## TAD Stability and Residual Gas

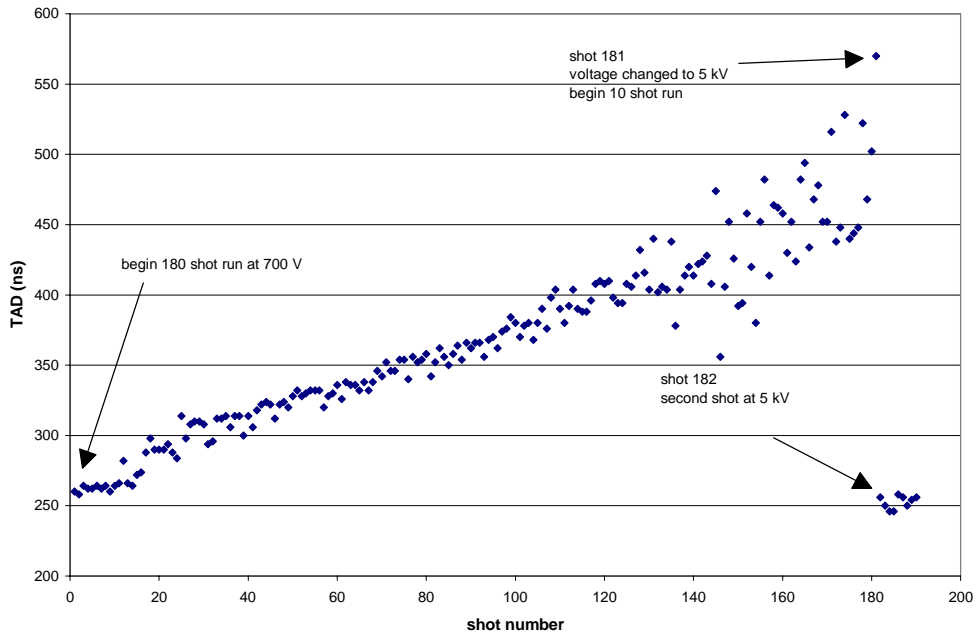
If the amount of residual gas fluctuates, the stability of the trigger-to-anode delay will suffer. A switch that is subjected to repeated firings is a dynamic device. Some changes, such as electrode erosion, are irreversible and accumulative; but other changes, such as residual gas, are partially reversible, and a repeatable pattern of behavior can be discerned. The amount of residual gas changes in response to temperature and to the intensity of the electric arc. For example, heat releases trapped gas and shortens the TAD. On the other hand, the electric arc may both release and remove gas. If one repeatedly fires a switch under the same conditions, the switch eventually reaches a point of equilibrium where gas release balances gas removal, and the TAD becomes stable. If conditions suddenly change, the residual gas is no longer in equilibrium, and the TAD will shift as the residual gas pressure changes. For example, increased current tends to release more gas and shift the equilibrium point toward shorter delay. If an application requires accurate timing, delay shifts caused by fluctuations of the residual gas pressure should be evaluated.

Figure 27 is an example of an unstable switch that shows clear evidence of residual gas. Prior to shot number 1, the switch had already been fired 170 times and had reached stability at 5 kV. At shot 31, we decreased the operating voltage to 3 kV, which caused TAD2 to gradually increase throughout the next 100 shots until it was five times its former value. We reset the voltage to 5 kV on shot 131, and TAD2 remained unchanged. However, TAD2 abruptly decreased on shot 132, and it stayed low during the remainder of the 20-shot run at 5 kV. Continuing with the experiment, we dropped the voltage back to 3 kV on shot 151 for a 40-shot run, effectively removing residual gas. After shot 190, we heated the switch by touching the anode and cathode with a hot soldering iron. After the switch returned to room temperature, we resumed the test at 3 kV, and TAD2 dropped abruptly on shot 191. It appears that either heat or higher peak current will quickly release trapped gas. Alternately, it requires many shots at reduced peak current to scavenge the same amount of gas.



**Figure 27. Residual Gas and Delay Instability.** Residual gas may reduce the stability of the vacuum switch. Gas may be released or removed when the operating voltage changes to higher or lower levels. Also, heating the switch may release gas. Having reached a stable TAD2 at 5 kV, the operating voltage was lowered to 3 kV on shot 31. TAD2 gradually increased for the next 100 shots at 3 kV. On shot 131, the voltage was brought back to 5 kV. Note that the delay for shot 131 remained unchanged; but on the next shot, the delay suddenly dropped, returning to its former value for 5 kV operation. The sudden decrease of TAD2 on shot 191 demonstrates that heating can also release gas.

The initial turn-on characteristics of the current waveform provide more evidence of residual gas. We fired a switch 180 times at 500 V (700 A peak current), expecting TAD to increase as the residual gas decreased (see Figure 28). On shot 181, we increased the voltage to 5 kV, beginning a ten-shot run. The delay remained long on shot 181, but shot 182 had a dramatically shorter delay (see Figure 29). In addition to delay time, the current waveforms differ substantially. The start of the current pulse on shot 181 is erratic and indicative of a higher vacuum. The smooth but abrupt turn-on of shot 182 is indicative of residual gas.



**Figure 28. Gas Removal.** Gas is continually removed for 180 shots by firing a vacuum switch at 700 V in a 0.2  $\mu\text{F}$  overdamped circuit (700 A peak current). On shot 181, the voltage increased to 5000 V, and the intense electric arc (8000 A peak current) released the trapped gas with this single shot. On shot 182, TAD was restored to its value at the start of the test.

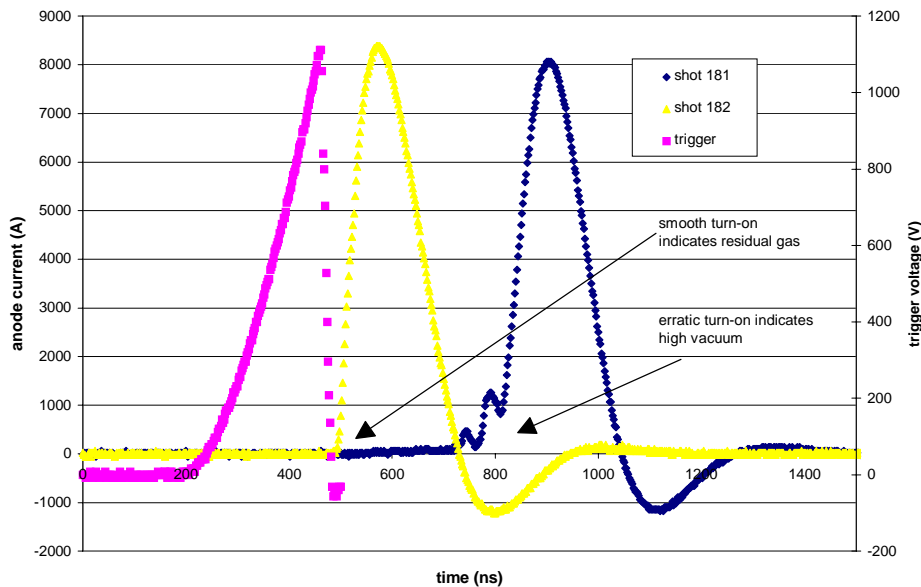


**Figure 29. Residual Gas and Current Pulse Shape.** The initial turn-on of the current pulse is dependent on the amount of residual gas. This graph shows shots 181 and 182 referenced in Figure 28, corresponding to little residual gas, has a rather erratic initial turn-on. Shot 182, with gas released by the previous shot, is very smooth. The two trigger pulses are nearly identical; for clarity, only the trigger pulse for shot 181 is shown.

## Early Isolated Hold-Off Failures

One of the most vexing issues surrounding vacuum switches is the early isolated hold-off failure. This type of failure is rare, with no precursory warning. The failure occurs well before the expected life of the switch and occurs only one time. And following the failure, the switch functions normally for hundreds or perhaps thousands of cycles. Interestingly, the cause of the failure is destroyed by the electric discharge that is generated by the failure.

To investigate these isolated hold-off failures, we modified the normal pulse-life test to measure the leakage current after each shot. We hoped that an anomalous leakage current might presage a failure and allow us to study the cause. Out of a dozen commercial switches, we found one instance of an isolated hold-off failure. This switch discharged a 0.2  $\mu\text{F}$  capacitor charged to 3000 V and produced a 7500 A current pulse. This switch suffered one hold-off failure after shot 13, but it then operated flawlessly out to 538 shots. At this point, the switch suffered three closely spaced hold-off failures, and we terminated the test. Figure 30 shows the TAD and the leakage current for the first 100 shots. We measured the leakage current at 3000 V bias with a 100 M $\Omega$  current-limiting resistor. Nothing unusual was observed, either before or after the hold-off failure; and this early isolated hold-off failure remains enigmatic.

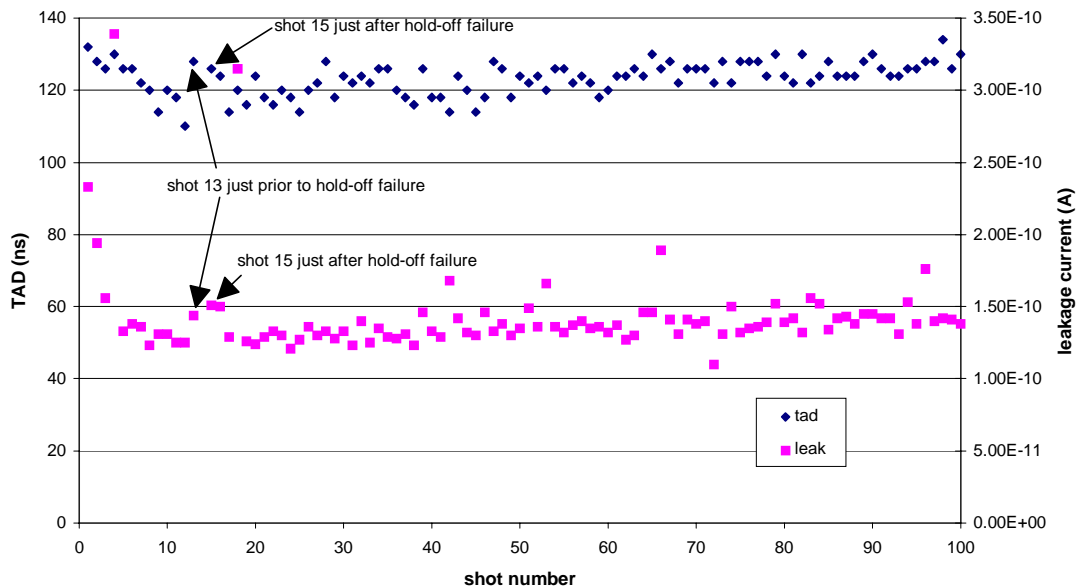


**Figure 30. Isolated Hold-Off Failure on Shot 14.** We measured the leakage current after each shot in an attempt to better understand isolated hold-off failures. This vacuum switch suffered a hold-off failure on shot 14, and then continued to operate with no more problems for over 500 shots. TAD and leakage current were normal immediately before and after the failure.

There are two leading explanations of vacuum breakdown: *microprotrusions* and *microparticles*.<sup>7</sup> According to the first explanation, a microprotrusion enhances the electric field, and the increased field emission heats the microprotrusion to a point of

instability, forming a microplasma. By the second explanation, loosely adhering microparticles are accelerated across the anode-cathode gap and on impact vaporize, producing a microplasma. In both explanations, the microplasma is the “seed” that eventually results in vacuum breakdown. The absence of an increased leakage current prior to the hold-off failure favors the microparticles explanation, which is also consistent with single failures since the microparticles are destroyed by the failure.

## Gap Erosion and Metal Deposition

The electric arc can simultaneously erode material from one region while it deposits material in another region. This is a very dynamic process where erosion or deposition may dominate, depending on the operating conditions. The greatest impact is on the trigger gap where plasma is first produced. Erosion can widen the gap, increasing trigger-break voltage; or deposition can narrow the gap, decreasing trigger-break voltage. This process is most readily apparent in a carbon-free switch that is triggered by breaking down a small gap spanned by a ceramic insulator (see Figure 31). Low-current pulses favor metal deposition in the trigger gap (decreasing the trigger-break voltage), and high-current pulses favor gap erosion (increasing the trigger-break voltage). The dynamic interplay between erosion and deposition of material within the trigger gap is responsible for many of the aging affects that are seen in vacuum switches.

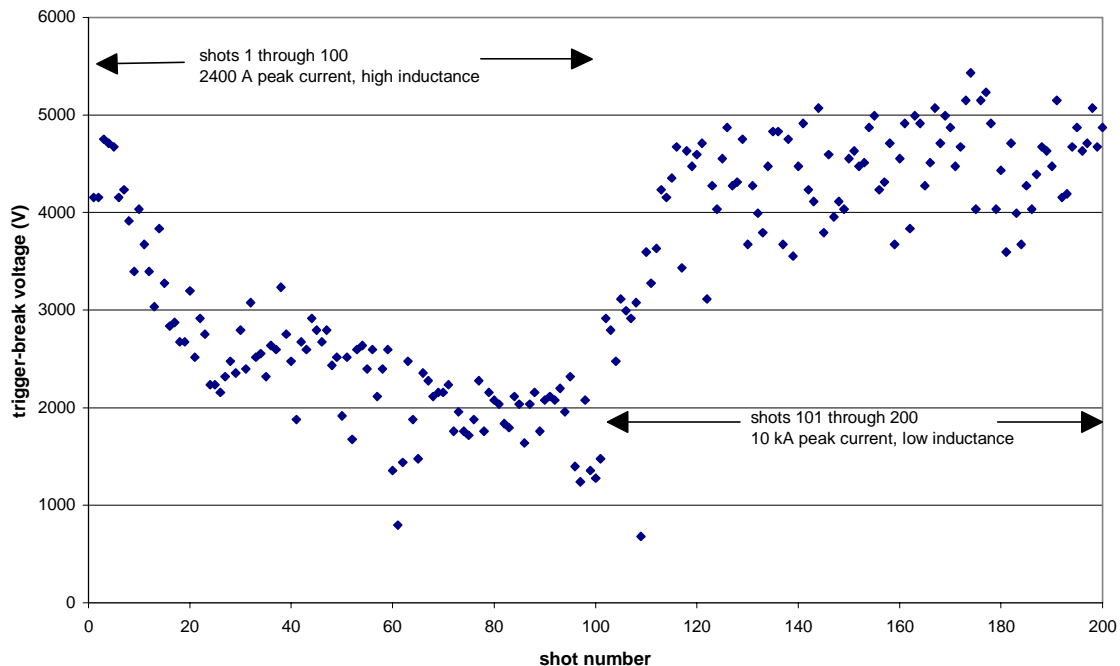


**Figure 31. Erosion and Deposition.** Electrical breakdown of a small gap was the trigger mechanism for this vacuum switch. Depending on operating conditions, this gap could be widened through erosion, or it could be narrowed through deposition of metal. This graph illustrates that at low currents sputtering dominates and the trigger-break voltage dropped to 2 kV. At high currents, erosion dominates, and the trigger-break voltage increased to 4.5 kV.

# Semiconductor Switches

The semiconductor industry has made great strides in recent years; and one new device, the metal oxide semiconductor (MOS)–controlled thyristor (MCT),<sup>8</sup> has performance that equals the best vacuum switches in capacitor-discharge circuits. The replacement of gas or vacuum switches by a semiconductor switch offers several benefits: much-improved stability, greater reliability, lower cost, and simpler triggering. For all practical purposes, a semiconductor switch is unchanged from shot to shot; and the current pulses exhibit a high degree of repeatability that cannot be achieved with gas or vacuum switches. By itself, this high stability provides only limited benefits; but the enhanced reliability, which results from high stability, is extremely important when dealing with fuzes. Semiconductor fabrication, a mainstream global technology, provides an inherent cost advantage over the small technological base for manufacturing gas and vacuum switches. Finally, a digital logic gate can directly drive a semiconductor switch, reducing cost and improving reliability.

The development of power-semiconductor switches is being driven by the needs of the electrical-power industry. To date, however, the semiconductor switches have not been optimized for capacitor-discharge circuits. For the control of electric power, turn-off of a switch when a large current is flowing is a more important issue than switch turn-on. Heat dissipation is a major problem for power control, but in a fuze the duty cycle is negligible. In a capacitor-discharge circuit, minimization of switch inductance and maximization of peak-current capability are the dominant considerations that govern package design. As this technology matures, MCT switches that are optimized for capacitor-discharge circuits will eventually become available.

Ongoing work to develop other high-speed power semiconductors may eventually provide alternatives to the MCT. One company is developing a high-speed thyristor,<sup>9</sup> and another company is improving the speed of the power metal oxide semiconductor field-effect transistor (MOSFET).<sup>10</sup> Although we have tested several other semiconductors, these switches are not included in this report. Currently, the MCT is so superior to the other semiconductors that it would be pointless to include these other devices.

## MCT Overview

Harris Semiconductor Corporation developed the MCT, with the majority of funding from the Office of Naval Research.<sup>11</sup> In November 1998, however, the MCT technology was transferred to Silicon Power Corporation. The primary application of the MCT is electrical-power control. Each MCT switch consists of tens of thousands of unit cells connected in parallel. Each unit cell consists of a thyristor and a pair of complementary MOSFETs, one for turn-on and the other for turn-off (see Figure 32). The MCT comes in two complementary versions, a P-MCT and an N-MCT. The MCT prefix identifies the turn-on MOSFET. In the P-MCT, a P-MOSFET turns on the device. In an N-MCT, an N-MOSFET turns on the device. For capacitor-discharge circuits, the N-

MCT is preferred because it offers faster turn-on. We tested N-MCT switches in two packages: a standard TO-218 plastic package and a proprietary low-inductance package, the thin pack. The latter package provides the better performance. All the data in this report was taken from either size-8 die (400 mil by 600 mil) mounted in a thin pack or size-6 die (260 mil by 390 mil) mounted in a TO-218 package.

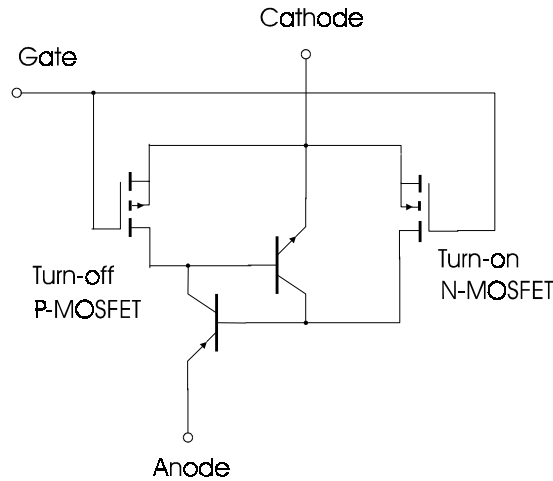


**Figure 32. N-MCT Diagram.** The electrical equivalent of a unit cell consists of a thyristor (represented by a two-transistor model) that is coupled to a P-MOSFET for turn-off and to an N-MOSFET for turn-on. One die typically contains many tens of thousands of unit cells. In the thin-pack package, stripline connections are directly soldered to the die, thereby avoiding small bond wires. This greatly enhances high-peak-current tolerance and simultaneously lowers switch inductance.

## N-MCT Stability

At a constant temperature, a semiconductor has excellent stability that is unmatched by gas or vacuum switches. This stability is readily demonstrated by a two-month pulse-life test on an N-MCT that spanned 274,000 shots. The N-MCT switch discharged a 0.4  $\mu\text{F}$  capacitor at 1200 V to produce a ringing current pulse with an 8.1 kA peak current. Figures 33 and 34 are histograms of the TAD and of the peak current for the first 1000 shots and the last 1000 shots. There is no significant difference between the beginning and the end of the test. Furthermore, the precision of test instruments (8-bit digitizer sampling at a 2 ns interval) is comparable to the data variance, and much of the variance in Figures 33 and 34 can be attributed to instrument limitations.

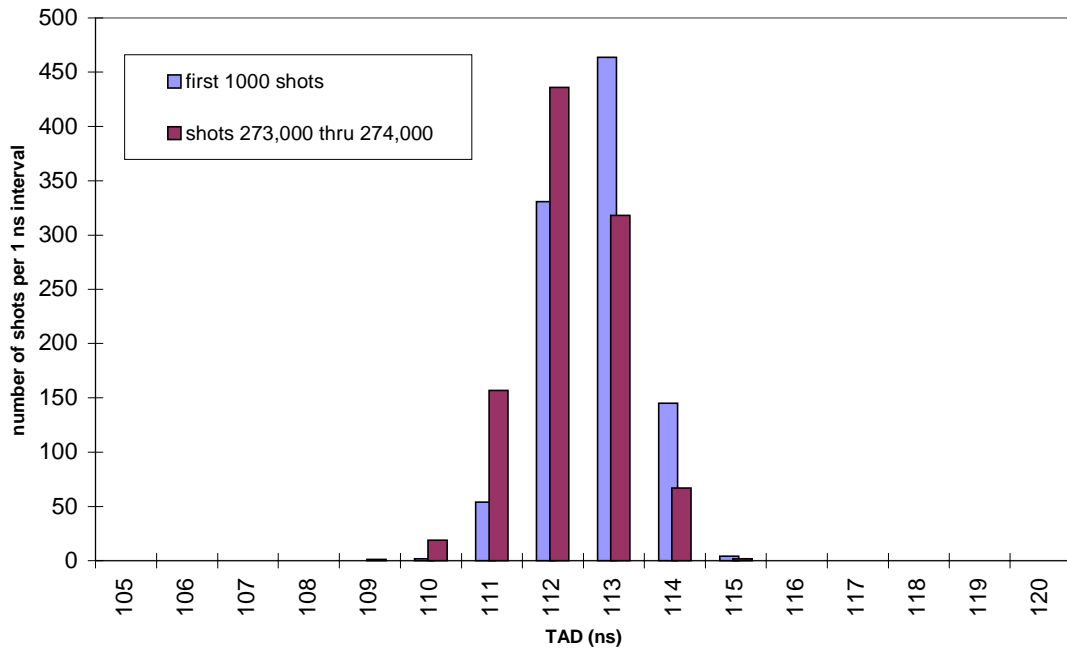


**Figure 33. TAD Histogram.** The switching delay of the N-MCT was stable throughout a 274,000-shot pulse-life test. The switch discharged a 0.4  $\mu\text{F}$  capacitor charged to 1200 V, producing an 8 kA ringing current pulse. The TAD histograms of the first 1000 shots and the last 1000 shots show no appreciable difference. The digitizer sampled at a 2 ns interval, and much of the timing deviation is related to test equipment limits as opposed to intrinsic N-MCT timing jitter.

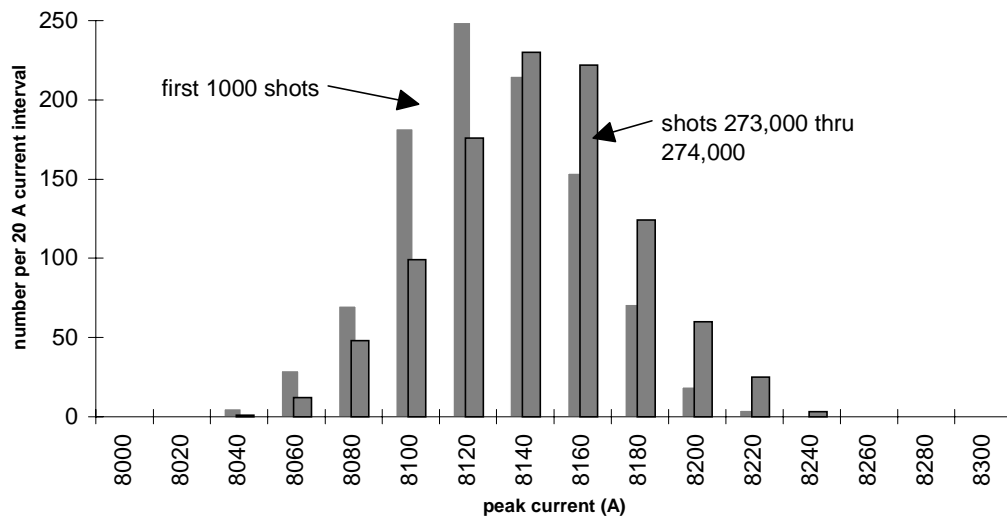


**Figure 34. Peak Current Temperature.** The peak current also has no appreciable shift from the beginning to the end of the 274,000-shot pulse-life test. The digitizing resolution was roughly 1% or 80 A, and much of the current deviation is a result of test equipment resolution as opposed to erratic switch performance.

Semiconductors are often sensitive to temperature variations. In our tests, the N-MCT was the only component inside the temperature chamber; everything else remained at room temperature. We fired the N-MCT ten times at each temperature, spanning the

–60°C to +100°C temperature range. Figure 35 shows TAD versus temperature, and Figure 36 shows peak current versus temperature. The small TAD shift with temperature, about 0.04 ns/°C, is insignificant for most applications. The peak current decreased with increasing temperature; but the total change was modest, about a 10% drop between –60°C and +100°C. The stability of the N-MCT switch was excellent, and it should be adequate for most fuze applications.

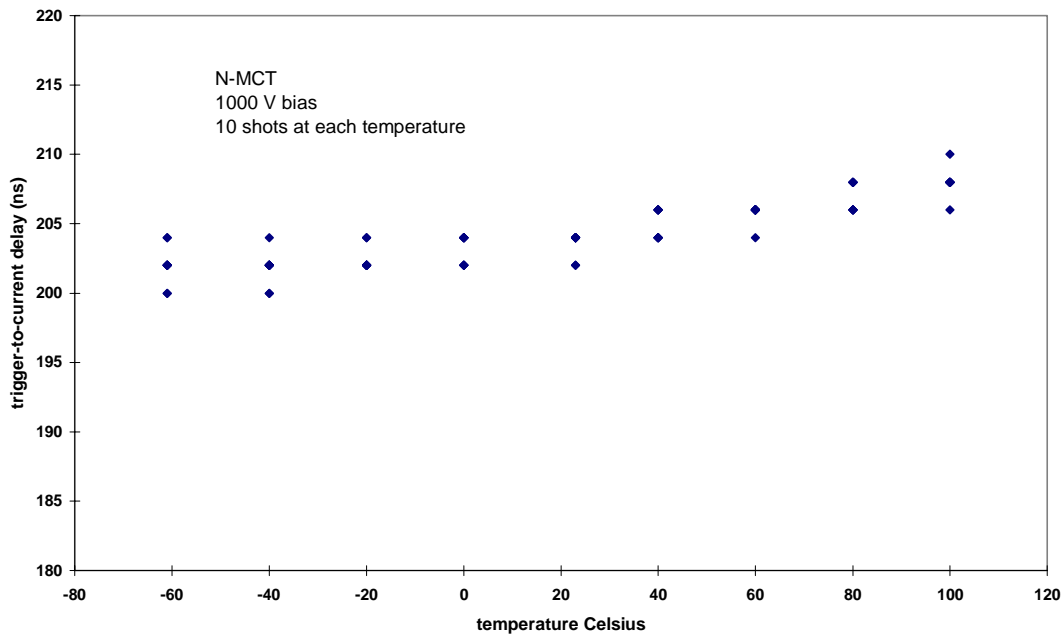


**Figure 35. TAD versus Temperature.** Over the temperature range of –60°C to +100°C, the TAD shift is only 10 ns. The switch discharged a 0.2 μF capacitor charged to 1000 V. This level of timing stability is excellent and is sufficient to meet most fuze requirements.

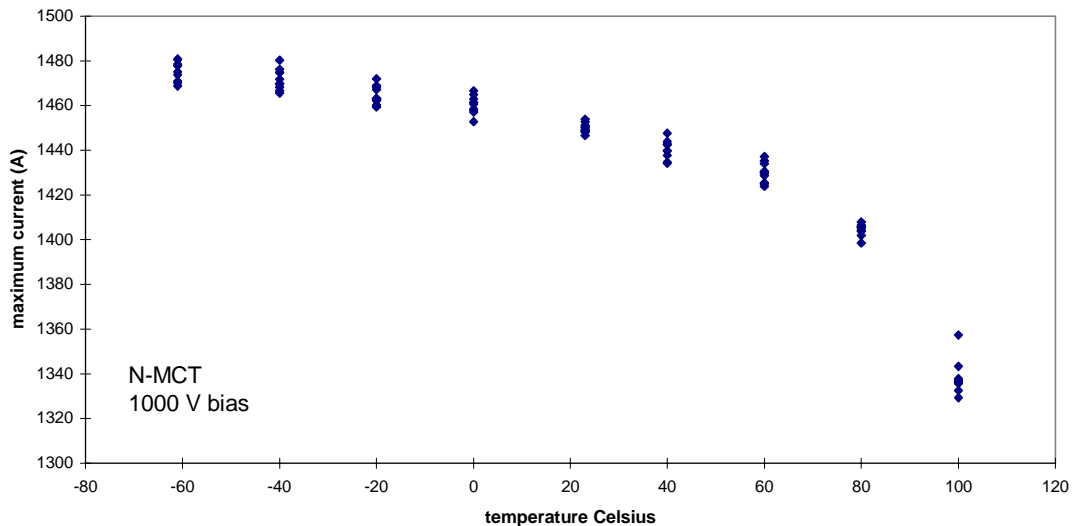


**Figure 36. Peak Current versus Temperature.** Over the temperature range of –60°C to +100°C, the peak current decreases by 10%. Most of the current degradation occurs at the high temperatures: +60°C to +100°C. This data comes from the same test as in Figure 35.

## N-MCT Leakage

We measured the leakage current of an N-MCT from  $-60^{\circ}\text{C}$  to  $+100^{\circ}\text{C}$  at a constant 1000 V bias (see Figure 37). At temperatures greater than  $0^{\circ}\text{C}$ , the current increases exponentially. If we were to extrapolate the leakage current up to  $200^{\circ}\text{C}$ , the switch would undoubtedly fail from thermal runaway (0.08 A leakage or 80 W at 1 kV). The N-MCT is not well suited for operation much above  $100^{\circ}\text{C}$ . Going toward cold temperatures, the leakage current does not drop much below 10 nA. The leakage current as a function of bias voltage is shown in Figure 38. We did not go above 1400 V because this N-MCT breaks down somewhere around 1500 V.

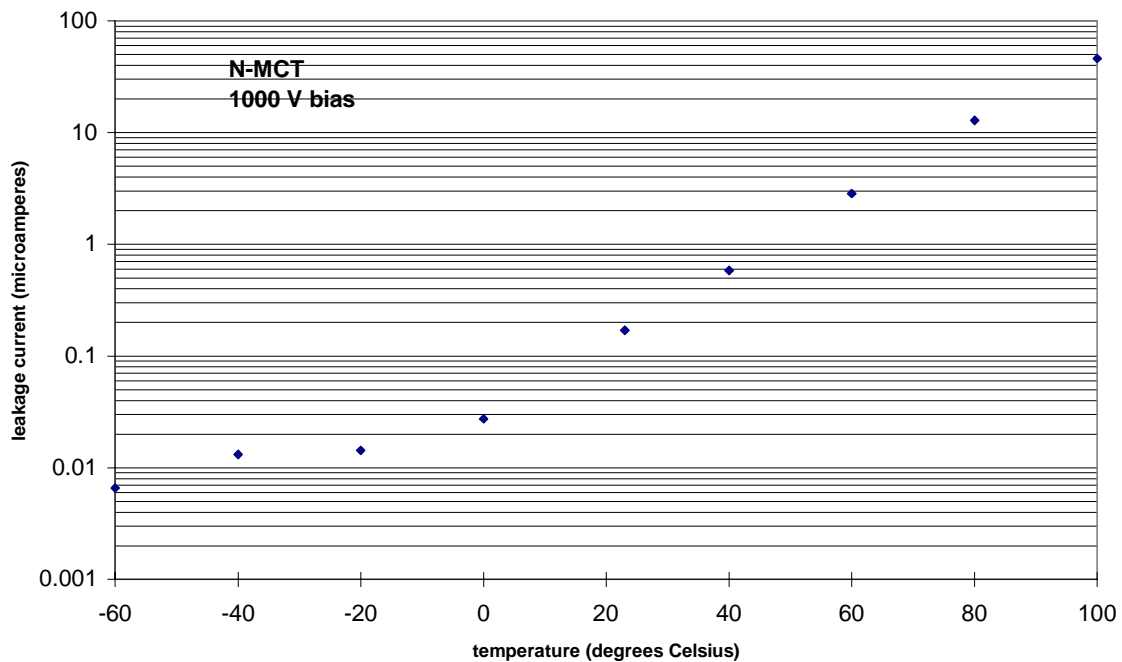


**Figure 37. Leakage Current versus Temperature.** For  $0^{\circ}\text{C}$  and higher, the leakage current increases exponentially with temperature, as expected for a p-n junction. For temperatures less than  $0^{\circ}\text{C}$ , we would assume some alternative leakage path begins to dominate over the p-n junction, keeping the leakage close to 10 nA.

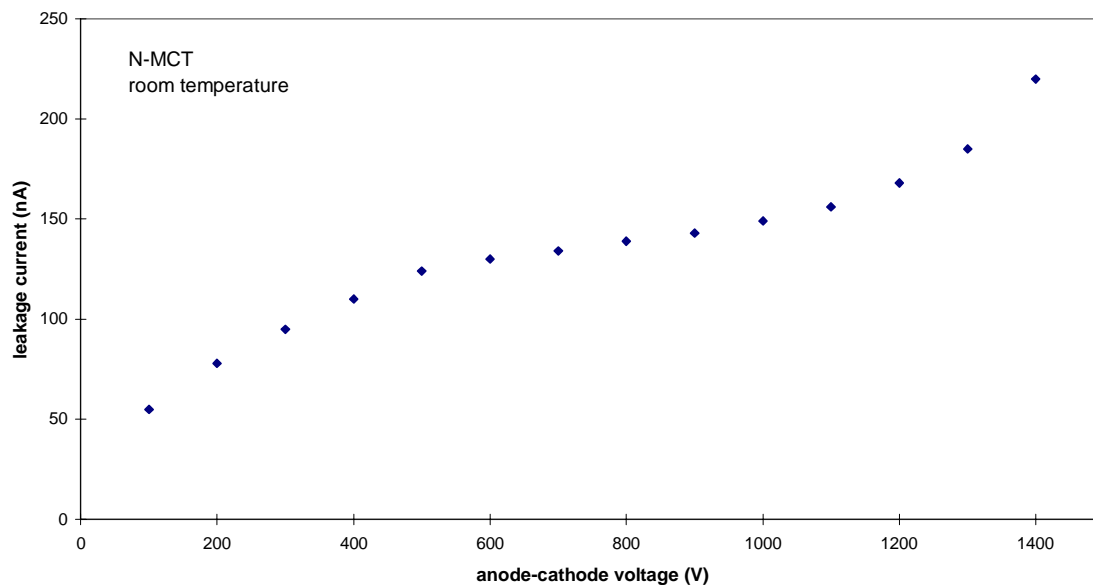


**Figure 38. Leakage Current versus Voltage.** The leakage current of the N-MCT is not a linear function of bias voltage. This particular device had a breakdown voltage around 1500 V; therefore, we limited the bias voltage in this test to 1400 V.

## Gate Protection

The gates of semiconductors are vulnerable to damage in capacitor-discharge circuits that produce very high  $dI/dt$ . Three major problems need to be considered: (1) uniform turn-on of the entire die, (2) premature turn-off caused by the main discharge current, and (3) gate breakdown caused by main discharge current. If a small region of the die carries a disproportionately large current, localized heating may damage the switch. This type of damage arises when the trigger fails to uniformly turn on the entire die. A low-impedance high-slew-rate trigger will mitigate this problem by causing the switch to transition from turn-off to turn-on as rapidly as possible. The second and third problems are caused by stray inductance that is common to the trigger loop and to the main-discharge loop. The preferable solution is to minimize this common inductance, but it cannot be completely eliminated. Driven by the high  $dI/dt$  of the main current pulse, the common stray inductance induces an additional current through the trigger loop. For some switches, the leading edge of the discharge current induces a current that tends to turn off the switch, possibly causing switch failure. In other switches, the induced current may lead to excessive gate voltage and possibly gate breakdown.

To illustrate these problems, we fired an N-MCT with a low-impedance, high-slew-rate trigger circuit (see Figure 39). A current-viewing transformer directly measured the gate current, but we calculated the gate voltage by integrating the gate current. There are several noteworthy observations (see Figure 40). The gate current is highly asymmetric, i.e., mostly positive. The silicon-controlled rectifier (SCR) in the trigger circuit readily

conducts current only in one direction: switch turn-on. The SCR is beneficial in preventing premature switch turn-off. On the other hand, the SCR is detrimental with respect to excessive gate voltage. In this ringing circuit, the voltage ratchets up to 50 V, well beyond the +15 V trigger supply voltage. The SCR readily allows the gate to charge to higher voltages, but it does not allow the gate to readily discharge. At 50 V, the gate is in great danger of breakdown (gate rated at 20 V).

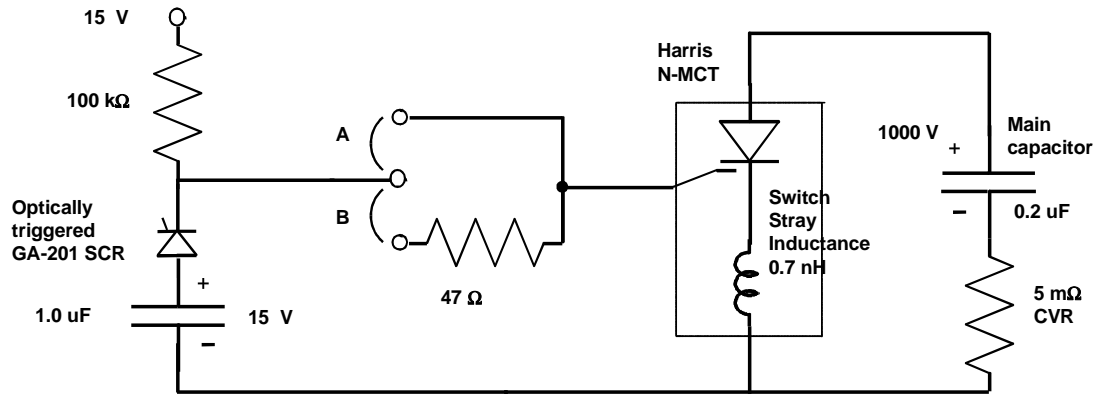


**Figure 39. N-MCT Trigger Circuit.** This trigger circuit illustrates the use of resistors to protect the gate. With no added resistance (jumper A), the trigger-slew rate is high, but the main discharge pulse induces large current flows in the trigger loop. By adding 47 Ω of resistance (jumper B), the trigger slew rate is low, but the main discharge pulse only induces negligible current flows.

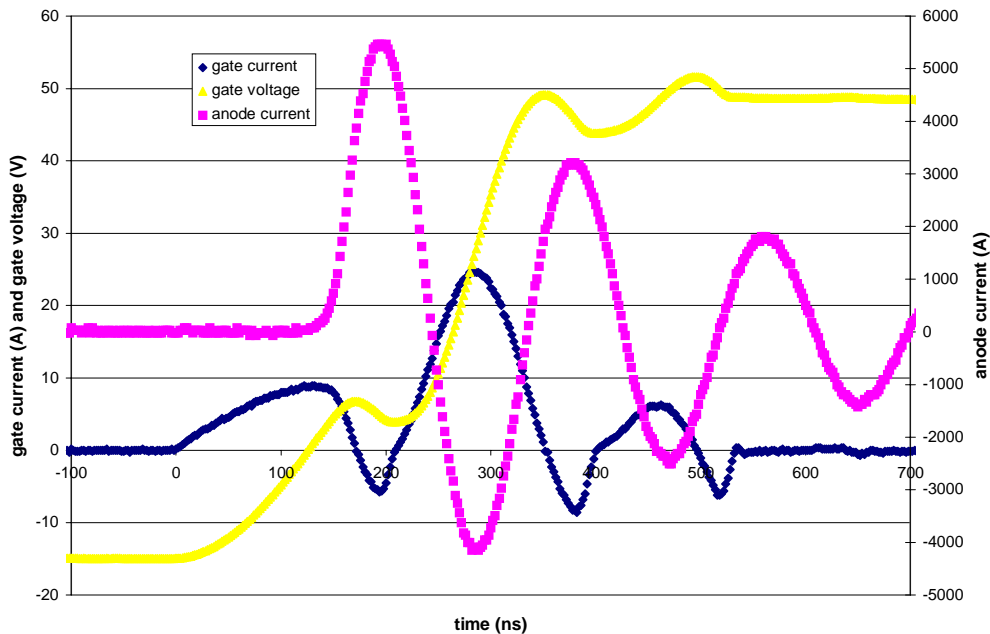


**Figure 40. Gate Overvoltage in Low-Impedance Trigger Circuit.** This figure shows the consequences of selecting the low-impedance option (jumper A in Figure 39). [Note that the GA201 SCR favors current flowing in the forward direction.] The negative portions of the ringing discharge circuit are effective in driving the gate voltage higher, but the positive portions of the ringing discharge circuit are ineffective in driving the gate voltage lower. Thus, the gate voltage ratchets up to 50 V, placing the gate in imminent danger of breakdown.

Adding  $47\ \Omega$  of resistance in the trigger loop eliminates the gate overvoltage problem (see Figure 41). The added resistance reduces the trigger slew-rate at the turn-on threshold from  $180\ \text{V}/\mu\text{s}$  to  $8\ \text{V}/\mu\text{s}$ , and the trigger current induced by  $dI/dt$  is reduced by a factor of 10 (compare Figures 42 and 43). The anode current did not change. The gate voltage now asymptotically approaches  $+15\ \text{V}$ , and the anode current produces only minor perturbations of the gate voltage. We fired the N-MCT with even higher resistance in the trigger circuits and determined that the N-MCT works well if the gate slew rate exceeds  $1\ \text{V}/\mu\text{s}$ . A possible disadvantage is that TAD increases from about  $100\ \text{ns}$  to well over  $1\ \mu\text{s}$  going from the low-resistance to the high-resistance trigger circuit.

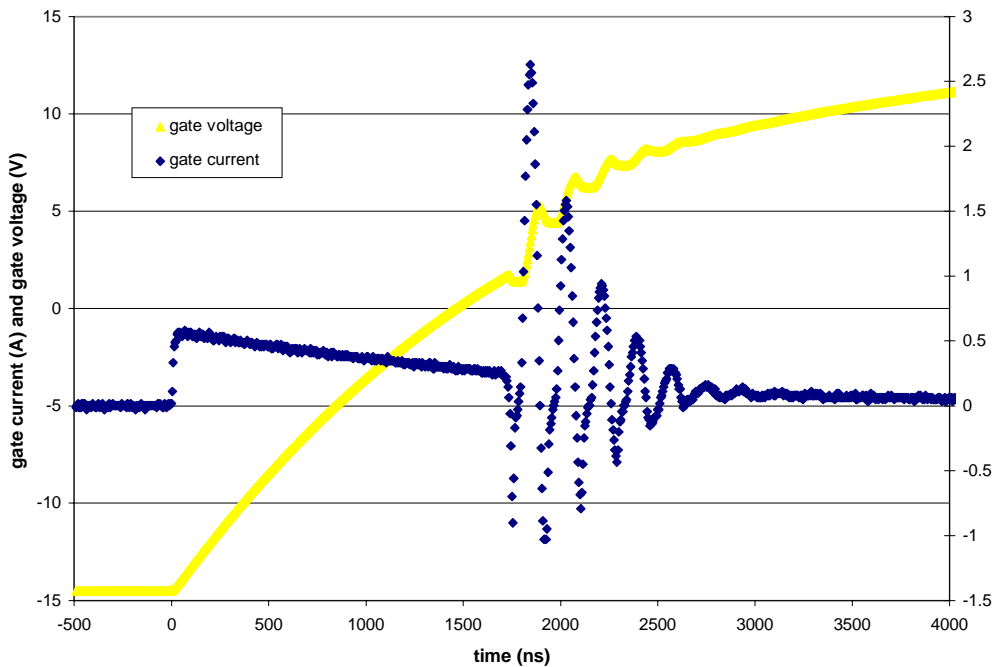


**Figure 41. Gate Protected in High-Impedance Trigger Circuit.** The resistance of the trigger circuit is increased by the addition of  $47\ \Omega$  (jumper B in Figure 39). At the price of a much longer TAD, the gate voltage remains below  $15\ \text{V}$ , a safe limit. Note the difference in time and voltage scales between Figures 40 and 41.

## Summary

Table 1 is a qualitative comparison of the three switch technologies. Although the N-MCT is currently the only viable semiconductor switch, alternative semiconductors may eventually be developed. The numbers in Table 1 are intended to be rough approximations and should not be construed as precise values.

**Table 1. Switch Comparisons**

Property	Gas Switches	Vacuum Switches	Semiconductor Switches (N-MCT)
Pulse-Life	Limited 100s to 1000s of shots	Limited 100s to 1000s of shots	Unlimited, tested to 50 million @ 8 kA
Timing accuracy	10 ns difficult 50 to 100 ns typical*	10 ns difficult 50 to 100 ns typical	2 ns @ fixed temperature 10 ns @ -60°C to +100°C
Stability	Possible first-shot effect Gas scavenged by arc Aging effects	Possible first-shot effect Possible residual gas Aging effects	Excellent
Operating voltage	1000 V to 5000 V typical	1000 V to 5000 V typical	Less than 1200 V
Peak current capability	Up to 10 kA typical**	Up to 10 kA typical**	20 kA for 400 x 600 mil die
Temperature	-60°C to above +200°C	-60°C to above +200°C	-60°C to +100°C
Cost	\$5 to \$200 for switch plus trigger circuit	\$50 to \$500 for switch plus trigger circuit	\$5 to \$40 for switch no dedicated trigger circuit
Abuse*** tolerance	High	High	Low
Radiation tolerance	Low	High	Low
Trigger requirements	1 kV or greater pulse	100 V or greater pulse	Logic gate compatible
Leakage	< 1 nA at operating voltage	< 1 nA at operating voltage	About 10 nA at 23°C About 10 µA at 80°C

\* depends on how close the operating voltage approaches the SBV

\*\* depends on required shot life and size of tube

\*\*\* examples of abuse include reverse bias, anode-cathode overvoltage, trigger overvoltage

All the switches were fired in the same test circuit to compare their switching performance. Peak current and  $dI/dt$  are plotted for several switches in Figures 42 and 43 at 1 kV and 3 kV, respectively. To put the data into proper perspective, we also plotted the theoretical peak current and  $dI/dt$  for a perfect switch (no inductance, no resistance, instantaneous turn-on) given the RLC of the test circuit (20 mΩ, 3.6 nH, 0.2 µF).

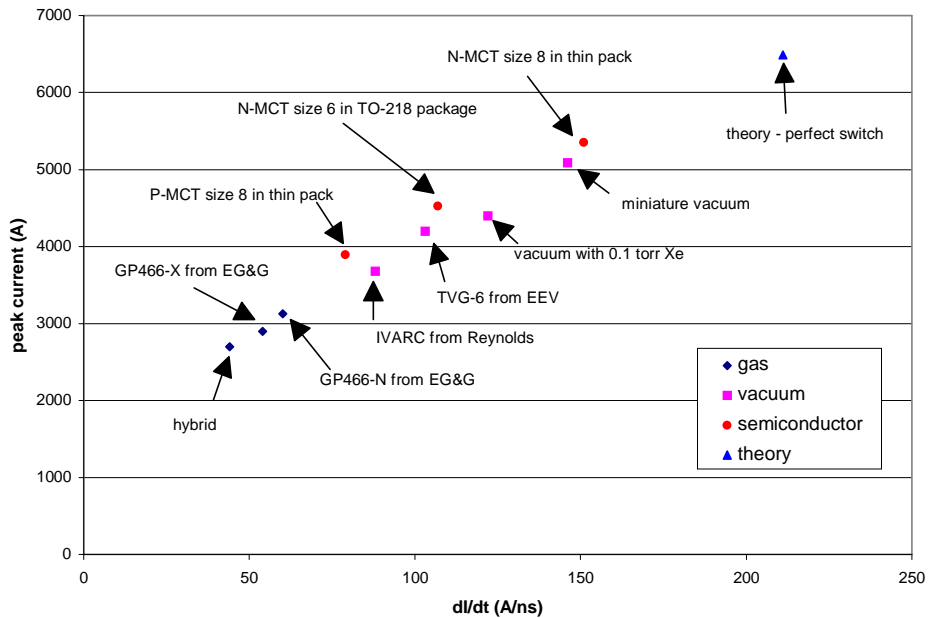


**Figure 42. Switching Performance at 1000 V.** We compared switching performance by plotting peak current and  $di/dt$ . All switches were fired at 1000 V in the same test circuit (i.e., RLC of 0.02  $\Omega$ , 3.6 nH, and 0.2  $\mu\text{F}$  in the absence of a switch). The performance of a theoretically perfect switch was calculated assuming a switch with zero resistance, zero inductance, and instantaneous turn-on.

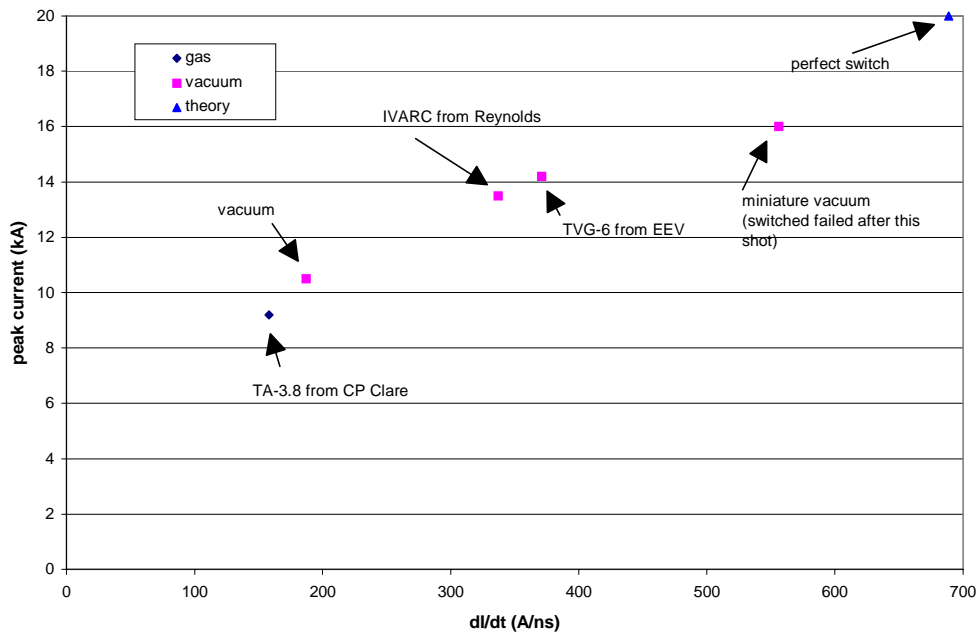


**Figure 43. Switching Performance at 3000 V.** This figure is the same as Figure 42 except that the operating voltage was at 3 kV. We did not test any semiconductor switches at 3 kV.

For the switches in Figures 42 and 43, Table 2 gives their inductance, turn-on time, and resistance. The resistance is defined as the value at peak current. We defined turn-on

time as the time for the resistance to drop from 1  $\Omega$  to 0.1  $\Omega$ . Turn-on time and resistance depend on the operating voltage, but inductance is independent of operating voltage.

**Table 2. Switch Inductance, Turn-On Time, and Resistance**

Switch	L nH	T ns @ 1 kV	R m $\Omega$ @ 1 kV	T ns @ 3 kV	R m $\Omega$ @ 3 kV
Gas, hybrid switch		56	100		
Gas, GP466, xenon fill, EG&G	4.3	73	130		
Gas, GP466, nitrogen fill, EG&G	4.4	51	75		
Gas, TA3.8, CP Clare	6.2			46	60
Vacuum, IVARC, Reynolds Industries	3.6	33	60	13	28
Vacuum, TVG6, EEV	2.0	18	40	8	20
Vacuum, Sandia design	5.5			30	35
Vacuum, Sandia design (0.1 torr Xe)	3.3	5	28		
Vacuum, Sandia design, miniature	1.6	9	15	8	10
Semiconductor, P-MCT, size 8, TP	0.5	15	20		
Semiconductor, N-MCT, size 6, TO-218	2.5	12	7		
Semiconductor, N-MCT, size 8, TP	0.5	11	10		

L = inductance of the switch

T = time for resistance to drop from 1  $\Omega$  to 0.1  $\Omega$

R = resistance at peak current

The market for fast-closing, low-inductance switches is at a crossroad. Vacuum and gas switches have long dominated capacitor-discharge applications, but recently the MCT has emerged with switching performance equal to the best vacuum switches. At the moment, the MCT is limited to 1200 V operation; but switches operating in the 3 to 4 kV range are possible, and efforts are being made to fabricate higher voltage switches. Currently, the MCT is not a developed commercial product, but the long-term advantages of semiconductor switches over vacuum and gas switches are tremendous. The manufacturing base of the MCT is a MOSFET fabrication line, a global mainstream technology; consequently, the MCT will have a large cost advantage over gas and vacuum switches. A solid-state switch does not wear out, and its stability greatly exceeds that of gas and vacuum switches. Unlimited pulse-life will open new applications that could not be done with gas or vacuum switches. Fuze applications, which do not require long pulse-life, will benefit from increased reliability. We believe that the advantages of a solid-state switch are overwhelming, and the real issue is “when” rather than “if” a semiconductor switch will take over much of the capacitor-discharge market.

Despite the many advantages of a semiconductor switch, there are three areas in which vacuum and gas switches will remain unchallenged by semiconductors for the foreseeable future: (1) high-temperature operation, (2) low-leakage current, and (3) radiation hardness (vacuum only). The leakage current of a semiconductor increases exponentially with temperature, and a semiconductor switch is probably limited to about 100°C, unless new semiconductors such as silicon carbide become practical. The temperature limit on a vacuum or gas switch is the braze temperature used to seal the tube. The braze temperature can be as high as 1000°C for some switches. Being essentially an open circuit, the leakage current of gas and vacuum switches is much

smaller than 1 nA at operating voltage. In the case of vacuum switches, they do not reach 1 nA of leakage current until voltage is several times greater than the nominal operating voltage. Furthermore, the vacuum switch is inherently radiation hardened; that is, there is no significant amount of ionizable matter within the anode-cathode gap. To the extent that there are applications where high temperature, low leakage, or radiation hardness are the preeminent concerns, vacuum and gas switches will continue to have a niche market.

## References

1. P. W. Cooper and S. R. Kurowski, *Introduction to the Technology of Explosives*, VCH Publishers, Inc., New York, NY, 1996.
2. J. M. Meek and J. D. Craggs, *Electrical Breakdown of Gases*, John Wiley & Son, New York, NY, 1989.
3. T. J. Williams, *The Theory and Design of the Triggered Spark Gap*, Sandia National Laboratories Report, SCTM 186-59-(14), May 22, 1959.
4. P. Osmokrovic and I. Krivokapic, "Mechanism of Electrical Breakdown Left of the Paschen Minimum," *IEEE Transactions of Dielectrics and Electrical Insulation*, Vol. 1, p. 77, February 1994.
5. G. Boettcher, "Cold Cathode Discharge Tube," U.S. patent 5,739,637, April 14, 1998.
6. S. Anders and B. Juttner, "Influence of Residual Gases on Cathode Spot Behavior," *IEEE Transactions of Plasma Science*, Vol. 19, p. 705, October 1991.
7. R. Latham, *High-Voltage Vacuum Insulation*, Academic Press, San Diego, CA, 1995.
8. V. A. K. Temple, "PEBB Devices and Device Physics," Available: <http://pebb.onr.navy.mil/techpaper.nsf>
9. A. H. Craig, D. C. Hopkins, and J. C. Driscoll, "A High-Speed Pulser Thyristor," *Proceedings of the 1998 IEEE Applied Power Electronics Conference*, Anaheim, CA, February 15–19, 1998.
10. Introduction to the DE-Series MOSFET Transistor, Available: <http://www.dirnrg.com>
11. Power Electronic Building Blocks (PEBB) Web Site, Available: <http://pebb.onr.navy.mil>

## Distribution

1	MS0311	G. E. Clark, 2674
10	MS0311	G. L. Scott, 2671
1	MS0311	G. R. Lyons, 2671
1	MS0311	J. W. Hole, 2671
1	MS0311	M. J. DeSpain, 2671
1	MS0311	R. P. Roberts, 2671
1	MS0328	J. A. Wilder, 2674
1	MS0328	P. A. Smith, 2674
1	MS0328	S. Holswade, 2674
1	MS0328	T. Mittas, 2674
1	MS0328	W. C. Curtis, 2674
1	MS0501	F. R. Trowbridge, 2674
1	MS0501	G. E. Boettcher, 2671
20	MS0501	K. W. Chu, 2671
1	MS0501	M. E. Smith, 2674
1	MS0501	R. R. Soutar, 2674
1	MS0507	C. Hart, 2600
1	MS0603	R. J. Shul, 1713
1	MS0619	Review & Approval Desk, 15102 for DOE/OSTI
1	MS0859	L. M. Wells, 2691
1	MS0860	B. Gomez, 2673
1	MS0860	M. A. Grohman, 5336
1	MS0860	V. C. Rimkus, 2673
2	MS0899	Technical Library, 4916
1	MS1453	W. W. Tarbell, 1553
1	MS9018	Central Technical Files, 8940-2